Input output selection based on worst case uncertainty

Input Output Selection Based on Worst Case Uncertainty

Marc van de Wal

WFW report 97.015

MARC VAN DE WAL
Faculty of Mechanical Engineering
Eindhoven University of Technology
April 1997

Input Output Selection Based on Worst Case Uncertainty

Marc van de Wal

Faculty of Mechanical Engineering
Eindhoven University of Technology
Eindhoven, The Netherlands

April 15, 1997

Abstract

Selection of control actuators and sensors aimed at Robust Performance (RP) is an important issue. This Input Output (IO) selection could be based on μ-synthesis, which is generally time-consuming. The basic idea of a new and more efficient IO selection method is to get rid of the structure of the combined uncertainty/performance block Δ arising in RP control problems. For this purpose, the concept of Worst Case Uncertainty (WCU) is introduced. This is the smallest uncertainty (in $\mathcal{H}_\infty$ norm sense), that violates the considered RP requirement.

The IO selection method proceeds as follows. First, an optimal μ-synthesis is performed including all actuators and sensors (full IO set). Second, for the closed-loop, WCU data is generated across a frequency grid. Third, a representative, real-rational, proper, and stable transfer function matrix is constructed for this data. Fourth, this (possibly structured) WCU representation is absorbed into the generalized plants for other IO sets and the structured Δ reduces to an unstructured performance block. Finally, IO selection amounts to checking criteria for the existence of a stabilizing controller achieving a specified closed-loop $\mathcal{H}_\infty$ norm. From previous research it is known, that this can be performed efficiently.

The proposed IO selection method relies on a necessary condition and IO sets may be incorrectly accepted. This necessity is due to two distinct sources. First, the WCU representation may considerably differ from the WCU data. As a result, the WCU representation may not be worst case for all frequencies, not even for the full IO set on which it is based. Second, even if the WCU representation is perfect for the full IO set, it may not be for other IO sets. While an unstable WCU representation may be easily constructed for the WCU data, a suitable stable one may not be possible. Therefore, a few construction procedures are discussed which impose stability at the price of dropping, *e.g.*, the perfect phase approximation.

Actuator and sensor selection for an active suspension is used as an example to evaluate the effectiveness and efficiency of the IO selection method. It appeared, that only one of the proposed WCU constructions could be applied "successfully." On the one hand, for this specific problem the IO selection method is ineffective. For a weak RP level requirement, many IO sets are incorrectly accepted, but the results are better for a strong RP level requirement. A remaining question is, if this can be concluded in general. On the other hand, for the application the IO selection method is considerably more efficient than IO selection based on μ-synthesis. Therefore, combining the necessity-based method from this report with a sufficiency-based method from previous research and μ-synthesis provides an effective and expectedly efficient approach to IO selection.

Contents

Chapter 1

Introduction

Preceding the design of a controller, it must be decided on an appropriate number, placement, and type of actuators (inputs) and sensors (outputs). This process will be called Input Output (IO) selection and each possible combination of inputs and outputs is called an IO set. Various IO selection methods are surveyed in [16]. Compared to other stages in control system design, IO selection has attracted little attention. Nevertheless, IO selection is crucial, since the IO set may put fundamental limitations on the achievable performance. It also affects control system complexity, hardware expenses, maintenance, and reliability. If the number of candidate IO sets is large, a systematic IO selection method could be invoked to complement the designer's experience and physical insight into the system and to avoid overlooking favorable candidates. For a quick evaluation of IO sets, such a method should be *efficient*. It should also be *effective*, in the sense that all IO sets are designated for which the intended objectives can and cannot be met.

In this report, a new IO selection method for *linear* control systems is proposed. The *goal* is to find those IO sets for which there exists a controller achieving a desired level of Robust Performance (RP). Such IO sets are termed *viable*. From a practical viewpoint, the viable IO set(s) with the fewest actuators and sensors may be preferred. The question if an IO set is viable could be answered by μ-synthesis. However, a more efficient approach to IO selection is desirable, since the number of candidate IO sets can be huge and a single μ-synthesis requires quite some time. Other known IO selection methods aimed at RP are also based on necessary conditions (like the LMI-approach in [8, 12, 15]), or on sufficient conditions (like the D-scale-estimate approach in [15, 18]).

The basic idea of the method presented here is to get rid of the structure in the combined uncertainty/performance block, which arises in RP control problems. For an unstructured block (*e.g.*, for nominal performance), IO selection can be performed efficiently by checking $\mathcal{H}_\infty$ controller existence conditions for each IO set as in [14, 17]. The suggested IO selection method involves four steps. First, μ-synthesis is performed for the full IO set including all candidate actuators and sensors. Second, for the resulting closed-loop and a specified frequency grid, data is generated for the smallest uncertainty which violates RP. This uncertainty will be called *"Worst Case Uncertainty (WCU)."* Third, a real-rational, proper, and stable ($\mathcal{RH}_\infty$) transfer function matrix is constructed to represent the WCU data. This uncertainty representation is finally absorbed into the generalized plants for the other IO sets and under the remaining unstructured performance block, the $\mathcal{H}_\infty$ controller existence conditions are checked.

The report is organized as follows. The background of the WCU is detailed in Chapter 2 and the new IO selection method is proposed in Chapter 3. Different ways to construct $\mathcal{RH}_\infty$ representations are discussed in Chapter 4. The IO selection relies on necessity, so nonviable IO sets may be accepted. This shortcoming is illustrated for an active suspension application in Chapter 5. In Chapter 6, conclusions on the usability of the method are drawn and some remaining questions are put forward.

Chapter 2

Worst Case Uncertainty

Before the IO selection method is presented in Chapter 3, the concept of WCU arising in complex structured singular value (μ) theory is introduced for matrices in Section 2.1. The use of μ for control problems is dealt with in Section 2.2. The consequences of absorbing a real-rational, proper, and stable WCU representation into the plant are addressed in Section 2.3.

2.1 μ and Worst Case Uncertainty for Matrices

In this section, the structured singular value μ is treated as a matrix function operating on complex matrices $M \in \mathbb{C}^{n \times m}$ (see, *e.g.*, [10]). In the definition of μ, there is an underlying structure $\mathbf{\Delta}$, which is a set of block diagonal matrices. Here, $\mathbf{\Delta}$ is restricted to be made up of *full complex* blocks, leaving out real and complex repeated blocks. This restriction avoids extra complications in the first exploration of the IO selection method and in the μ-synthesis for the full IO set. For a discussion on control system analysis and design for more general $\mathbf{\Delta}$ structures, it is referred to [20] (μ-analysis) and [19] (μ-synthesis). For the matrix feedback connection in Fig. 2.1, the following structures are considered:

$$\begin{aligned}
\mathbf{\Delta_u} &= \left\{\Delta_u = \text{diag}(\Delta_{u_1}, \ldots, \Delta_{u_k}) : \; \Delta_{u_i} \in \mathbb{C}^{m_i \times n_i}\right\}, \\
\mathbf{\Delta_p} &= \left\{\Delta_p : \; \Delta_p \in \mathbb{C}^{m_l \times n_l}\right\}, \qquad (2.1) \\
\mathbf{\Delta} &= \left\{\Delta = \text{diag}(\Delta_u, \Delta_p) : \; \Delta \in \mathbb{C}^{m \times n}\right\},
\end{aligned}$$

with:

$$m_l + \sum_{i=1}^{k} m_i = m \text{ and } n_l + \sum_{i=1}^{k} n_i = n. \qquad (2.2)$$

In case of control system design, the *structured* block Δ_u accounts for modeling uncertainties, while the *unstructured* fictitious block Δ_p accounts for performance specifications, see Section 2.2. Note, that each block in Δ is allowed to be nonsquare. Often, norm bounded

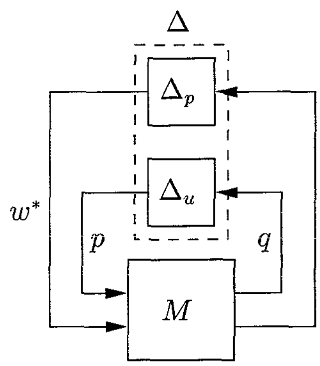

Figure 2.1: Matrix interconnection with $w = \binom{p}{w^*}$ and $z = \binom{q}{z^*}$

subsets are used:

$$\begin{aligned} \boldsymbol{B}_{\boldsymbol{\Delta}_u} &= \{\Delta_u \in \boldsymbol{\Delta}_u : \ \bar{\sigma}(\Delta_u) \leq 1\}, \\ \boldsymbol{B}_{\boldsymbol{\Delta}_p} &= \{\Delta_p \in \boldsymbol{\Delta}_p : \ \bar{\sigma}(\Delta_p) \leq 1\}, \\ \boldsymbol{B}_{\boldsymbol{\Delta}} &= \{\Delta \in \boldsymbol{\Delta} : \ \bar{\sigma}(\Delta) \leq 1\}, \end{aligned} \tag{2.3}$$

with $\bar{\sigma}$ the largest singular value of a matrix. The structured singular value μ is defined as follows, see, *e.g.*, [10]:

Definition of μ: *Given a matrix $M \in \mathbb{C}^{n \times m}$ and a compatible block diagonal structure $\boldsymbol{\Delta}$, the structured singular value $\mu_{\boldsymbol{\Delta}}(M)$ of M with respect to $\boldsymbol{\Delta}$ is defined as:*

$$\mu_{\boldsymbol{\Delta}}(M) := \frac{1}{\min_{\Delta \in \boldsymbol{\Delta}} \{\bar{\sigma}(\Delta) : \ \det(I - M\Delta) = 0\}}, \tag{2.4}$$

unless no $\Delta \in \boldsymbol{\Delta}$ makes $I - M\Delta$ singular, in which case $\mu_{\boldsymbol{\Delta}}(M) := 0$.

It is instructive to give a "feedback" interpretation of the μ definition [10]. Consider Fig. 2.1, which represents the loop equations $z = Mw$ and $w = \Delta z$. As long as $I - M\Delta$ is nonsingular, the only solutions z and w to these equations are $z = w = 0$. However, if $I - M\Delta$ is singular there are infinitely many solutions and the norms of z and w can be arbitrarily large. Motivated by connections with dynamic systems, the constant matrix feedback system in Fig. 2.1 is called "unstable." Likewise, the system is "stable" when the only solutions are zero. Thus, $\mu_{\boldsymbol{\Delta}}(M)$ provides a measure of the smallest structured Δ causing instability. The maximum singular value of this destabilizing Δ is exactly $1/\mu_{\boldsymbol{\Delta}}(M)$.

Exact computation of μ cannot be performed efficiently in general. Instead, μ is approximated by lower and upper bounds, which are based on the following inequalities:

$$\rho(M) \leq \mu_{\boldsymbol{\Delta}}(M) \leq \bar{\sigma}(M). \tag{2.5}$$

Since the gap between these bounds can be arbitrarily large, they are not directly suitable for μ computation. To (partially) solve this, transformations on M are used, which do not affect μ, but which do affect ρ and $\bar{\sigma}$. The upper bound will not be further discussed (see, *e.g.*, [10]), because only the lower bound is related to the IO selection method. For lower bound computation, the subset $\boldsymbol{Q}$ of $\mathbb{C}^{m\times n}$ is defined [10, 11]:

$$\boldsymbol{Q} = \{Q \in \boldsymbol{\Delta} : \; Q^*Q = I_n\}, \tag{2.6}$$

with Q^* the conjugate transpose of Q. The μ lower bound in (2.5) can now be tightened to give an exact expression for μ:

$$\mu_l(M) := \max_{Q\in\boldsymbol{Q}} \rho(MQ) = \mu_{\boldsymbol{\Delta}}(M). \tag{2.7}$$

Note, that the lower bound is actually an equality. Unfortunately, the quantity $\rho(MQ)$ can have multiple local maxima, which are not global. Thus, local search cannot guarantee to obtain μ, but can only yield a lower bound. Using the μ-Synthesis and Analysis Toolbox [1] (abbreviated "μ-Tools"), both upper and lower bounds for μ are computed with the function mu. Though for the lower bound there are open questions about convergence, it is stated in [1, Chapter 4], that the computation usually works quite well (at least for complex Δ). It is assumed in this report, that the μ lower bound exactly equals μ.

The minimum Δ from (2.4) making $I - M\Delta$ singular is denoted $\bar{\Delta}$ and plays a key role in the IO selection. Its corresponding uncertainty block $\bar{\Delta}_u$ will be referred to as the Worst Case Uncertainty (WCU) and is given an interpretation in Section 2.2. It is emphasized, that $\bar{\Delta}$ is not unique. Using the μ-Tools function mu, $\bar{\Delta}$ is obtained from the μ lower bound computation, see [10, Section 7] and [11]. For this construction, each diagonal block in $\bar{\Delta}$ has rank one and $\bar{\sigma}(\bar{\Delta}) = \bar{\sigma}(\bar{\Delta}_{u_1}) = \ldots = \bar{\sigma}(\bar{\Delta}_{u_k}) = \bar{\sigma}(\bar{\Delta}_p) = 1/\mu_l(M)$. Though the sub-blocks in $\bar{\Delta}_u$ and $\bar{\Delta}_p$ are not required to have the same norm, it is a legitimate and convenient property. Throughout the rest of this report, $\bar{\Delta}$ is assumed to be constructed with the μ-Tools algorithm and hence it is assumed to have the two properties mentioned above. Further details on the construction of $\bar{\Delta}$ are not figured out and could be further investigated.

It will now be shown how the WCU lays the foundation for the IO selection proposal. Consider Fig. 2.1, with M partitioned as:

$$z = \begin{bmatrix} q \\ z^* \end{bmatrix} = \begin{bmatrix} M_{11} & M_{12} \\ M_{21} & M_{22} \end{bmatrix} \begin{bmatrix} p \\ w^* \end{bmatrix} = Mw. \tag{2.8}$$

So, M_{11} and M_{22} correspond to the loops around Δ_u and Δ_p respectively. Closing M with Δ_u, w^* and z^* are related according to $z^* = \mathcal{F}_u(M, \Delta_u)w^*$, with the upper Linear Fractional Transformation (LFT):

$$\mathcal{F}_u(M, \Delta_u) := M_{22} + M_{21}\Delta_u(I - M_{11}\Delta_u)^{-1}M_{12}. \tag{2.9}$$

In the sequel, the "main loop theorem" plays an important role. This theorem is formulated below for structured Δ_p [10], which is a more general case than considered in the rest of the report:

Main Loop Theorem: *Let $\gamma > 0$ be given. Then:*

$$\mu_{\boldsymbol{\Delta}}(M) < \gamma \;\Leftrightarrow\; \begin{cases} \mu_{\boldsymbol{\Delta}_u}(M_{11}) < \gamma \\ \max_{\Delta_u \in (1/\gamma)\boldsymbol{B}_{\boldsymbol{\Delta}_u}} \mu_{\boldsymbol{\Delta}_p}(\mathcal{F}_u(M, \Delta_u)) < \gamma. \end{cases} \tag{2.10}$$

From the definition of μ, it can be verified that $\mu_{\mathbf{\Delta}_u}(M_{11}) \leq \mu_{\mathbf{\Delta}}(M)$, see also [21, Chapter 11]. Though possibly $\mu_{\mathbf{\Delta}_u}(M_{11}) = \mu_{\mathbf{\Delta}}(M)$, an essential *assumption* in this report is $\mu_{\mathbf{\Delta}_u}(M_{11}) < \mu_{\mathbf{\Delta}}(M)$. In the context of control system design, this implies that the robust stability problem is "easier" than the robust performance problem (which includes robust stability). The assumption simplifies the development of the theory and will generally be satisfied for practical problems. The following notion plays a key role in this report:

WCU Theorem: *Assume $\mu_{\mathbf{\Delta}_u}(M_{11}) < \mu_{\mathbf{\Delta}}(M)$, then the WCU $\bar{\Delta}_u$ satisfies the equality:*

$$\mu_{\mathbf{\Delta}}(M) = \bar{\sigma}(\mathcal{F}_u(M, \bar{\Delta}_u)) \tag{2.11}$$

and therefore (with γ a positive scalar):

$$\mu_{\mathbf{\Delta}}(M) < \gamma \;\Leftrightarrow\; \bar{\sigma}(\mathcal{F}_u(M, \bar{\Delta}_u)) < \gamma. \tag{2.12}$$

Proof: First, recall that $\bar{\Delta}$ is defined as a minimum Δ making $I - M\Delta$ singular and hence (according to the definition of μ) $\mu_{\mathbf{\Delta}}(M) = \frac{1}{\bar{\sigma}(\bar{\Delta})}$. The following can always be written:

$$\det(I - M\Delta) = \det\left(\begin{bmatrix} I - M_{11}\Delta_u & -M_{12}\Delta_p \\ -M_{21}\Delta_u & I - M_{22}\Delta_p \end{bmatrix}\right). \tag{2.13}$$

Under the assumption $\mu_{\mathbf{\Delta}_u}(M_{11}) < \mu_{\mathbf{\Delta}}(M)$, $I - M_{11}\Delta_u$ is nonsingular for all $\Delta_u \in \bar{\sigma}(\bar{\Delta})\boldsymbol{B}_{\mathbf{\Delta}_u}$. Invoking Schur formulas (see [21, Section 2.3]), equality (2.13) can be rewritten as follows for $\Delta \in \bar{\sigma}(\bar{\Delta})\boldsymbol{B}_{\mathbf{\Delta}}$:

$$\begin{aligned} \det(I - M\Delta) &= \det(I - M_{11}\Delta_u)\det(I - M_{22}\Delta_p - M_{21}\Delta_u(I - M_{11}\Delta_u)^{-1}M_{12}\Delta_p) \\ &= \det(I - M_{11}\Delta_u)\det(I - \mathcal{F}_u(M, \Delta_u)\Delta_p). \end{aligned} \tag{2.14}$$

For the considered Δ, $\det(I - M_{11}\Delta_u)$ is never zero and so the left hand side is zero if and only if $\det(I - \mathcal{F}_u(M, \Delta_u)\Delta_p) = 0$. The fact that $\bar{\Delta} = \text{diag}(\bar{\Delta}_u, \bar{\Delta}_p)$ is a smallest Δ for which $I - M\Delta$ is singular implies, that the block $\bar{\Delta}_p$ with $\bar{\sigma}(\bar{\Delta}_p) = \bar{\sigma}(\bar{\Delta})$ is a smallest Δ_p for which $I - \mathcal{F}_u(M, \Delta_u)\Delta_p$ is singular for all $\Delta_u \in \bar{\sigma}(\bar{\Delta})\boldsymbol{B}_{\mathbf{\Delta}_u}$. Hence (compare with the main loop theorem):

$$\mu_{\mathbf{\Delta}}(M) = \max_{\Delta_u \in \bar{\sigma}(\bar{\Delta})\boldsymbol{B}_{\mathbf{\Delta}_u}} \mu_{\mathbf{\Delta}_p}(\mathcal{F}_u(M, \Delta_u)). \tag{2.15}$$

Now replace Δ_u and Δ in (2.14) by $\bar{\Delta}_u$ and $\left[\begin{smallmatrix} \bar{\Delta}_u & 0 \\ 0 & \Delta_p \end{smallmatrix}\right]$ respectively. Since $\bar{\Delta}_p$ is a smallest Δ_p for which $I - M\left[\begin{smallmatrix} \bar{\Delta}_u & 0 \\ 0 & \Delta_p \end{smallmatrix}\right]$ is singular, $\bar{\Delta}_p$ is also a smallest Δ_p for which $I - \mathcal{F}_u(M, \bar{\Delta}_u)\Delta_p$ is singular, *i.e.*:

$$\mu_{\mathbf{\Delta}}(M) = \mu_{\mathbf{\Delta}_p}(\mathcal{F}_u(M, \bar{\Delta}_u)). \tag{2.16}$$

Notice, that $\bar{\Delta}_u$ maximizes the right hand side of (2.15). The proof of (2.11) is completed by noting that $\mu_{\mathbf{\Delta}_p}(\cdot) = \bar{\sigma}(\cdot)$ for the unstructured Δ_p. Finally, (2.12) follows trivially from (2.11).

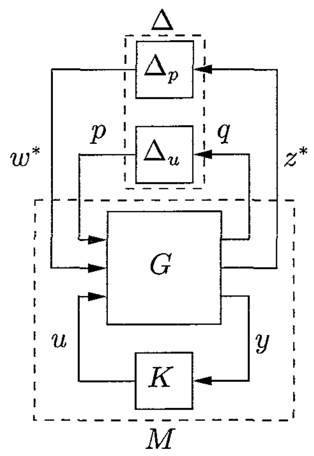

G	:	generalized plant	p	:	output from uncertainty block
K	:	controller	q	:	input to uncertainty block
M	:	generalized closed-loop	w^*	:	exogenous variables
Δ_u	:	uncertainty block	z^*	:	regulated variables
Δ_p	:	performance block	u	:	manipulated variables *(inputs)*
Δ	:	$\text{diag}(\Delta_u, \Delta_p)$	y	:	measured variables *(outputs)*

Figure 2.2: Standard control system set-up

2.2 μ and Worst Case Uncertainty for Control Systems

In this section, μ is treated for dynamic control systems. More details are given in [1, Chapter 4] and [21, Chapter 11]. Essentially, the standard control system set-up in Fig. 2.2 can be viewed as a dynamic equivalent of the constant matrix interconnection in Fig. 2.1. G is called the generalized plant, which includes nominal plant data and design filters. The latter reflect performance specifications and characterizations of exogenous variables and system uncertainties. These uncertainties are represented by the (possibly structured) block Δ_u, while a *fictitious* unstructured block Δ_p accounts for performance specifications. As in [21, Chapter 11], it is assumed, that Δ is in $\mathcal{RH}_\infty$, *i.e.*, Δ is real-rational, proper, and stable (real-rational functions are fractions of polynomials in a complex-valued variable s with real coefficients). The following sets now represent $\mathcal{RH}_\infty$ Transfer Function Matrices (TFMs), which are "dynamic versions" of the matrices in (2.1) and (2.3):

$$\begin{aligned} \mathcal{M}(\boldsymbol{\Delta}) &= \{\Delta \in \mathcal{RH}_\infty : \ \Delta(j\omega) \in \boldsymbol{\Delta} \ \forall \ \omega \in \mathbb{R}\} \, , \\ \mathcal{M}(\boldsymbol{B_\Delta}) &= \{\Delta \in \mathcal{RH}_\infty : \ \Delta(j\omega) \in \boldsymbol{B_\Delta} \ \forall \ \omega \in \mathbb{R}\} \, , \end{aligned} \tag{2.17}$$

Analogous definitions apply for the uncertainty block ($\mathcal{M}(\boldsymbol{\Delta_u})$ and $\mathcal{M}(\boldsymbol{B_{\Delta_u}})$) and for the performance block ($\mathcal{M}(\boldsymbol{\Delta_p})$ and $\mathcal{M}(\boldsymbol{B_{\Delta_p}})$). The generalized plant G and the controller K are assumed proper and real-rational with stabilizable and detectable state-space descriptions [21, Chapter 16]. Controllers with the additional property of being internally stabilizing are termed "*admissible*" [21, Chapter 16] and the set of all admissible controllers is denoted $\mathcal{K}_A$.

The generalized closed-loop M relating $w = \binom{p}{w^*}$ and $z = \binom{q}{z^*}$ is obtained by a lower LFT:

$$M = \mathcal{F}_l(G, K) := G_{11} + G_{12}K(I - G_{22}K)^{-1}G_{21}. \tag{2.18}$$

The partitioning of M is the same as for the constant matrix interconnection in (2.8) and G is partitioned as follows:

$$\begin{bmatrix} z \\ y \end{bmatrix} = \begin{bmatrix} G_{11} & G_{12} \\ G_{21} & G_{22} \end{bmatrix} \begin{bmatrix} w \\ u \end{bmatrix}. \tag{2.19}$$

With μ it is possible to test particular properties of the closed-loop M, *e.g.*, Robust Performance (RP). A control system is said to achieve RP if it is stable and meets the performance specifications in the presence of a class of uncertainties $\mathcal{M}(\boldsymbol{\Delta}_u)$. The performance requirement is expressed as an $\mathcal{H}_\infty$ norm bound on the TFM between w^* and z^*, *i.e.*, on the perturbed TFM $\mathcal{F}_u(M, \Delta_u)$. For a stable TFM T, the $\mathcal{H}_\infty$ norm is defined as follows, see, *e.g.*, [21, Chapter 4]:

$$\|T\|_\infty := \sup_\omega \bar{\sigma}(T(j\omega)). \tag{2.20}$$

The following provides a necessary and sufficient test for an RP level γ [21, Chapter 11]:

Robust Performance Theorem: *Let $\gamma > 0$ and let Δ_u and M in Fig. 2.2 be stable. For all $\Delta_u \in \frac{1}{\gamma}\mathcal{M}(\boldsymbol{B}_{\boldsymbol{\Delta}_u})$, the uncertain system $\mathcal{F}_u(M, \Delta_u)$ is stable and $\|\mathcal{F}_u(M, \Delta_u)\|_\infty < \gamma$, i.e., robust performance is achieved, if and only if:*

$$\|M\|_\mu < \gamma, \ \text{with } \|M\|_\mu := \sup_\omega \mu_{\boldsymbol{\Delta}}(M(j\omega)). \tag{2.21}$$

Testing condition (2.21) is referred to as μ-analysis, while designing a controller K such that (2.21) is met, or $\|M\|_\mu$ is minimized, is called μ-synthesis. For a more thorough treatment of μ-analysis and μ-synthesis in the case of complex Δ, see, *e.g.*, [21, Chapter 11]. In practice, μ-analysis is performed in an interesting frequency range for a finite number of frequencies ("frequency grid"). For a given frequency grid and closed-loop M, a smallest $\Delta(j\omega)$ making $I - M(j\omega)\Delta(j\omega)$ singular for *all* considered frequencies (not just one, which is, however, enough to violate RP) is denoted $\bar{\Delta}(j\omega)$, with $\bar{\sigma}(\bar{\Delta}(j\omega)) = 1/\mu_{\boldsymbol{\Delta}}(M(j\omega))$. Its sub-block $\bar{\Delta}_u$ is called a Worst Case Uncertainty, since it is a smallest uncertainty Δ_u for which $\bar{\sigma}(\mathcal{F}_u(M, \Delta_u)) = \mu_{\boldsymbol{\Delta}}(M)$, *i.e.*, for which the RP level $\gamma = \|M\|_\mu$ is violated.

2.3 Worst Case Uncertainty as Transfer Function Matrix

In this section, the focus is on representing the WCU data in $\bar{\Delta}_u(j\omega)$ by a real-rational, proper, and stable ($\mathcal{RH}_\infty$) transfer function matrix $\hat{\Delta}_u(s)$. As will become clear in Chapter 3, the motivation is to get rid of the structured Δ hampering IO selection, by absorbing $\hat{\Delta}_u(s)$ into the generalized plant G and leaving the unstructured performance block Δ_p alone. Throughout the rest of this report, it is *assumed* that all features which are crucial for the investigated problem are covered by the designer-specified frequency grid $\Omega = \{\omega_1, \ldots, \omega_N\}$. This is important for μ-synthesis and for the construction of meaningful WCU data.

By assuming $\mu_{\mathbf{\Delta}_u}(M_{11}(j\omega)) < \mu_{\mathbf{\Delta}}(M(j\omega))$ and applying (2.12) over the frequency grid Ω, the following is guaranteed:

$$\mu_{\mathbf{\Delta}}(M(j\omega)) < \gamma \; \forall \; \omega \in \Omega \;\Leftrightarrow\; \bar{\sigma}(\mathcal{F}_u(M(j\omega), \bar{\Delta}_u(j\omega))) < \gamma \; \forall \; \omega \in \Omega. \tag{2.22}$$

If $\bar{\Delta}_u(j\omega)$ is *perfectly* represented for all $\omega \in \Omega$ by a real-rational and proper $\hat{\Delta}_u(s)$, *i.e.*, $\hat{\Delta}_u(j\omega) = \bar{\Delta}_u(j\omega) \; \forall \; \omega \in \Omega$, the following is evident:

$$\mu_{\mathbf{\Delta}}(M(j\omega)) = \bar{\sigma}(\mathcal{F}_u(M(j\omega), \bar{\Delta}_u(j\omega))) = \bar{\sigma}(\mathcal{F}_u(M(j\omega), \hat{\Delta}_u(j\omega))) \; \forall \; \omega \in \Omega. \tag{2.23}$$

If this perfect representation is also stable (*i.e.*, $\hat{\Delta}_u \in \mathcal{RH}_\infty$) and if $\|\hat{\Delta}_u\|_\infty$ occurs inside Ω, the combination of (2.22) and (2.23) yields:

$$\|M\|_\mu < \gamma \;\Leftrightarrow\; \|\mathcal{F}_u(M, \hat{\Delta}_u)\|_\infty < \gamma. \tag{2.24}$$

Suppose M with $\|M\|_\mu < \gamma$ is given and the corresponding WCU data $\bar{\Delta}_u$ has a perfect $\mathcal{RH}_\infty$ representation $\hat{\Delta}_u$. According to (2.24), this implies the existence of an admissible controller K achieving $\|\mathcal{F}_l(\mathcal{F}_u(G, \hat{\Delta}_u), K)\|_\infty < \gamma$. If M results from an optimal μ-synthesis, hence $\|M\|_\mu = \beta$ cannot be reduced further, then also $\min_{K \in \mathcal{K}_A} \|\mathcal{F}_l(\mathcal{F}_u(G, \hat{\Delta}_u), K)\|_\infty = \beta$.

Now, *imperfect* WCU representations $\hat{\Delta}_u$ are considered, for which the following three assumptions must be met:

1. $\bar{\sigma}(\hat{\Delta}_u(j\omega)) \leq \bar{\sigma}(\bar{\Delta}_u(j\omega)) \; \forall \; \omega \in \Omega$. So, in the specified grid the magnitude of the WCU representation is never larger than the magnitude of the data.
2. $\|\hat{\Delta}_u\|_\infty := \sup_\omega \bar{\sigma}(\hat{\Delta}_u(j\omega)) \leq \sup_{\omega \in \Omega} \bar{\sigma}(\bar{\Delta}_u(j\omega))$. So, the magnitude of the WCU representation is not larger than the maximum magnitude of the WCU data in the considered grid.
3. $\|\mathcal{F}_u(M, \hat{\Delta}_u)\|_\infty \leq \sup_{\omega \in \Omega} \bar{\sigma}(\mathcal{F}_u(M, \bar{\Delta}_u))$. So, the magnitude of the perturbed closed-loop is not larger than $\|M\|_\mu$, which is assumed to be achieved in Ω.

Under these assumptions, the following inequality replaces (2.23):

$$\bar{\sigma}(\mathcal{F}_u(M(j\omega), \hat{\Delta}_u(j\omega))) \leq \bar{\sigma}(\mathcal{F}_u(M(j\omega), \bar{\Delta}_u(j\omega))) \; \forall \; \omega \in \Omega. \tag{2.25}$$

This is explained as follows. Recall, that $\bar{\Delta}_u(j\omega)$ is a maximizing uncertainty in the right hand side of (2.15). However, if $\hat{\Delta}_u(j\omega) \neq \bar{\Delta}_u(j\omega)$, the representation $\hat{\Delta}_u$ does not necessarily maximize the right hand side of (2.15) and (2.25) follows. So, for an imperfect $\hat{\Delta}_u$ which is not larger than $\bar{\Delta}_u$, there is a gap between $\mu_{\mathbf{\Delta}}(M)$ and $\bar{\sigma}(\mathcal{F}_u(M, \hat{\Delta}_u))$. Under the three assumptions listed above, the equivalences in (2.22) and (2.24) are now replaced by implications:

$$\mu_{\mathbf{\Delta}}(M(j\omega)) < \gamma \; \forall \; \omega \in \Omega \;\Rightarrow\; \bar{\sigma}(\mathcal{F}_u(M(j\omega), \hat{\Delta}_u(j\omega))) < \gamma \; \forall \; \omega \in \Omega, \tag{2.26}$$

$$\|M\|_\mu < \gamma \;\Rightarrow\; \|\mathcal{F}_u(M, \hat{\Delta}_u)\|_\infty < \gamma. \tag{2.27}$$

The main conclusion is, that $\|\mathcal{F}_u(M, \hat{\Delta}_u)\|_\infty < \gamma$ is *necessary* for $\|M\|_\mu < \gamma$ with an imperfect WCU representation $\hat{\Delta}_u$. So, an RP level $\|M\|_\mu < \gamma$ is possible *only if* for the generalized plant absorbing a $\hat{\Delta}_u$ meeting the three assumptions, there exists a controller achieving $\min_{K \in \mathcal{K}_A} \|\mathcal{F}_l(\mathcal{F}_u(G, \hat{\Delta}_u), K)\|_\infty < \gamma$.

Chapter 3

Input Output Selection Proposal

The WCU concept offers some prospects for IO selection. In analogy to the D-scale estimation approach to IO selection in [15,18], the effects of employing the WCU from the full IO set for other IO sets will be studied.

To start with, consider the *full IO set* for which the generalized plant and the closed-loop are denoted $G^\star$ and $M^\star$ respectively. Suppose $M^\star$ results from an optimal μ-synthesis, with $\|M^\star\|_\mu = \beta$ and corresponding WCU data $\bar{\Delta}_u(j\omega)$. This implies the following for all $\omega \in \Omega$:

$$\bar{\sigma}(\mathcal{F}_u(M^\star, \Delta_u)) \leq \beta \;\forall\; \Delta_u \in \mathcal{M}(\boldsymbol{\Delta}_u) \text{ with } \bar{\sigma}(\Delta_u(j\omega)) \leq \bar{\sigma}(\bar{\Delta}_u(j\omega)). \tag{3.1}$$

For the WCU data corresponding to $M^\star$, the following holds:

$$\frac{1}{\beta} = \min_{\omega\in\Omega} \bar{\sigma}(\bar{\Delta}_u(j\omega)) = \bar{\sigma}(\bar{\Delta}_u(j\omega_0)) \;\forall\; \omega \in \Omega_0, \tag{3.2}$$

with Ω_0 the frequencies (usually one) where $\mu_{\boldsymbol{\Delta}}(M^\star)$ is largest. So, the minimum magnitude of the WCU equals $\frac{1}{\beta}$ for $\omega \in \Omega_0$, but for other $\omega \in \Omega$ the magnitude of $\bar{\Delta}_u$ may be larger and even infinite. The following notion from the Robust Performance Theorem in Section 2.2 plays an important role throughout the rest of this chapter: for the optimal $M^\star$ with $\|M^\star\|_\mu = \beta$, there is a particular Δ_u in the set $\frac{1}{\beta}\mathcal{M}(\boldsymbol{B}_{\boldsymbol{\Delta}_u})$ for which the performance level β is not achieved, *i.e.*, there is a $\Delta_u \in \frac{1}{\beta}\mathcal{M}(\boldsymbol{B}_{\boldsymbol{\Delta}_u})$ for which $\bar{\sigma}(\mathcal{F}_u(M^\star, \Delta_u)) = \beta$.

Next, consider *subsets* of the full IO set. The lowest achievable $\|M\|_\mu$ values for these IO sets are larger than or equal to $\|M^\star\|_\mu = \beta$, since eliminating actuators and sensors will never improve the best achievable control (obviously, if β is larger than or equal to the RP requirement γ, the full IO set and its subsets are nonviable). This implies the following for the WCU data corresponding to the optimal closed-loops:

$$\frac{1}{\beta} = \bar{\sigma}(\bar{\Delta}_u(j\omega_0)) \;\forall\; \omega \in \Omega_0 \text{ for full IO set} \geq \min_{\omega\in\Omega} \bar{\sigma}(\bar{\Delta}_u(j\omega)) \text{ for other IO sets.} \tag{3.3}$$

In words: the minimum magnitude of the WCU for the full IO set is always larger than or equal to the minimum magnitude of the WCU for a different IO set. However, this remark may not hold true frequency-by-frequency, *i.e.*, for each $\omega \in \Omega$ (also for $\omega \in \Omega_0$) the WCU for the full IO set may be smaller than for a different IO set. It is emphasized, that the minimum magnitude of the WCU for a different IO set is not necessarily achieved for the same frequencies Ω_0.

Now, it will be shown how the WCU for the full IO set could be used to asses other IO sets. Recall from Section 2.3, that the existence of an admissible controller K achieving $\|\mathcal{F}_u(M^\star, \hat{\Delta}_u)\|_\infty < \gamma$ (with $\hat{\Delta}_u$ fulfilling the three assumptions) is necessary for the existence of a K achieving $\|M^\star\|_\mu < \gamma$. So, it is necessary for the full IO set to be viable with respect to the RP level γ. If a close-to-perfect $\mathcal{RH}_\infty$ representation $\hat{\Delta}_u \approx \bar{\Delta}_u$ were used, this condition would be tight (*i.e.*, almost necessary *and* sufficient) for the *full* IO set. As should be clear from (3.3) and the remark below (3.3), for other IO sets this $\hat{\Delta}_u$ may either be too large, or too small for particular frequencies. Hence, for other IO sets it is *a priori* unknown whether $\min_{K\in\mathcal{K}_A} \|\mathcal{F}_l(\mathcal{F}_u(G, \hat{\Delta}_u), K)\|_\infty < \gamma$ is a necessary or a sufficient condition for $\|M\|_\mu < \gamma$. This ambiguity is circumvented by using a WCU representation $\hat{\Delta}_u$ with $\|\hat{\Delta}_u\|_\infty = \frac{1}{\beta}$. So, $\hat{\Delta}_u \in \frac{1}{\beta}\mathcal{M}(\boldsymbol{B}_{\boldsymbol{\Delta}_u})$ and the condition is always necessary. Considered over the frequency grid, $\hat{\Delta}_u(j\omega)$ may be much smaller than $\bar{\Delta}_u(j\omega)$ for the full IO set. A few approaches to construct WCU representations are discussed in Chapter 4.

The resulting $\hat{\Delta}_u$ may still be outside the class of uncertainties $\frac{1}{\gamma}\mathcal{M}(\boldsymbol{B}_{\boldsymbol{\Delta}_u})$ the system is required to robustly perform against (*i.e.*, $\hat{\Delta}_u$ may still be too large), since it is based on WCU data $\bar{\Delta}_u$ from an *optimal* μ-synthesis: $\frac{1}{\beta} > \frac{1}{\gamma}$. Equivalently, the best achievable RP level with the full IO set may be larger than strictly required: $\beta < \gamma$. To resolve this, $\hat{\Delta}_u$ from the full IO set is scaled down by the factor $\frac{\beta}{\gamma} \leq 1$, so:

$$\tilde{\Delta}_u := \frac{\beta}{\gamma}\hat{\Delta}_u \in \frac{1}{\gamma}\mathcal{M}(\boldsymbol{B}_{\boldsymbol{\Delta}_u}). \tag{3.4}$$

The motivation to use $\hat{\Delta}_u$ from the full IO set for other IO sets is based on the following reasoning. The optimal M for an IO set which is "almost as good" as the full IO set will have approximately the same dynamic behavior as $M^\star$, *i.e.*, $M^\star(s) \approx M(s)$. As a result, $\mu_{\boldsymbol{\Delta}}(M^\star) \approx \mu_{\boldsymbol{\Delta}}(M)$ and the WCU data for $M^\star$ and M (if constructed with the same algorithm) are approximately the same. In that case, $\hat{\Delta}_u$ for the full IO set is also a good WCU representation for the other equally good IO sets, provided $\hat{\Delta}_u$ is a good representation of $\bar{\Delta}_u$ for the full IO set.

Define $\tilde{G} := \mathcal{F}_u(G, \hat{\Delta}_u)$ and $\tilde{M} := \mathcal{F}_l(\tilde{G}, K)$. The following IO selection method is now proposed:

IO Selection with Worst Case Uncertainty: *Consider Fig. 2.2 and the WCU representation $\hat{\Delta}_u$ corresponding to the full IO set's optimal closed-loop with $\|\hat{\Delta}_u\|_\infty = 1/\beta$. Assume $\gamma > \beta$. For each candidate IO set, the generalized plant with the down-scaled $\tilde{\Delta}_u$ absorbed into it is constructed and it is tested if there exists an admissible controller $K \in \mathcal{K}_A$ achieving $\|\tilde{M}\|_\infty < \gamma$. Since this is a necessary condition for existence of a $K \in \mathcal{K}_A$ achieving $\|M\|_\mu < \gamma$, IO sets which do not meet this condition are nonviable for the RP level γ.*

To check the existence of an admissible controller achieving $\|\tilde{M}\|_\infty < \gamma$, conditions involving the solutions to two algebraic Riccati equations are used. To apply the conditions, the state-space description of $\tilde{G}$ must satisfy the standard $\mathcal{H}_\infty$ assumptions (see, *e.g.*, [21, Chapter 17] and [14, Section 2.3]), which are usually not restrictive for practical problems. Some of these assumptions could be dropped if a linear matrix inequality approach were used instead, see, *e.g.*, [4]. The employed conditions are given a short interpretation here; for details, the reader is referred to [21, Chapter 16&17] and [14, Section 2.4]:

1. Check if the open-loop direct feed-through from w^* to z^* is not "too large," since K cannot completely cancel this effect.
2. Check if K with full information on w^* and the states of $\tilde{G}$ (ideal output set) meets $\|\tilde{M}\|_\infty < \gamma$.
3. Check if K with full access to z^* and the states of $\tilde{G}$ (ideal input set) meets $\|\tilde{M}\|_\infty < \gamma$.
4. Based on results from 2 and 3, check if the combination of input set and output set meets $\|\tilde{M}\|_\infty < \gamma$.

The candidate IO sets are subjected to these conditions, for which functions from μ-Tools [1] form the basis. As soon as one condition fails, the others need not be checked.

Due to the necessary character of the IO selection method, it may be ineffective: candidate IO sets may be incorrectly accepted. This necessity stems from two distinct sources. First, across the frequency grid, the WCU representation $\tilde{\Delta}_u$ for the full IO set may be "smaller" than the WCU data $\bar{\Delta}_u$. As explained above, this is due to the need for a WCU representation $\tilde{\Delta}_u$ that is in the relevant class of uncertainties $\frac{1}{\gamma}\mathcal{M}(\boldsymbol{B}_{\boldsymbol{\Delta}_u})$. Second, even if $\tilde{\Delta}_u$ were perfect for the full IO set, it may not be "as bad" as the true WCU representation for other IO sets. The necessity can also be interpreted by noting, that the WCU representation $\tilde{\Delta}_u$ is one specific uncertainty in the set $\frac{1}{\gamma}\mathcal{M}(\boldsymbol{B}_{\boldsymbol{\Delta}_u})$. However, the requirement $\|M\|_\mu < \gamma$ implies, that RP should be achieved against *all* uncertainties in this set. If $\tilde{\Delta}_u$ is not worst case $\forall\ \omega \in \Omega$, controller design for only $\tilde{\Delta}_u$ is easier than for all uncertainties in $\frac{1}{\gamma}\mathcal{M}(\boldsymbol{B}_{\boldsymbol{\Delta}_u})$.

The effectiveness of the IO selection method may deteriorate further if the variables in w and z are directly linked with u and y. First, this occurs for uncertainties in Δ_u, which are related to u or y, such as multiplicative and additive input and output uncertainties. Second, sensor noise and actuator weights may be contained in w^* and z^* respectively (connected via Δ_p). In these two cases, μ-synthesis for the full IO set accounts for additional control objectives compared to other IO sets. Consequently, the difference between the full IO set's $\hat{\Delta}_u$ and the WCU representations resulting from μ-syntheses for the other IO sets may become larger.

Chapter 4

Construction of WCU Representations

This chapter discusses a few approaches to generate $\mathcal{RH}_\infty$ representations for the WCU data $\bar{\Delta}_u$. Recall, that the μ lower bound is assumed to equal the exact μ. Suppose again, that the full IO set's closed-loop $M^\star$ results from an optimal μ-synthesis and that $\|M^\star\|_\mu = \beta$. The aim is to construct a suitable WCU representation $\hat{\Delta}_u \in \frac{1}{\beta}\mathcal{M}(\boldsymbol{B}_{\boldsymbol{\Delta}_u})$. If $\bar{\sigma}(\bar{\Delta}_u) = 1/\mu_{\boldsymbol{\Delta}}(M)$ is not flat across the frequency grid Ω, it makes no sense to approximate the magnitude of $\bar{\Delta}_u$, since the perfect $\hat{\Delta}_u$ would not be in the relevant set $\frac{1}{\beta}\mathcal{M}(\boldsymbol{B}_{\boldsymbol{\Delta}_u})$. Instead, modified data $\bar{\Delta}'_u$ with $\bar{\sigma}(\bar{\Delta}'_u) \le \frac{1}{\beta}\ \forall\ \omega \in \Omega$ should form the basis for IO selection.

The difference between $\bar{\sigma}(\mathcal{F}_u(M^\star, \hat{\Delta}_u))$ and $\bar{\sigma}(\mathcal{F}_u(M^\star, \bar{\Delta}_u))$ depends on the difference between the magnitude and phase of $\hat{\Delta}_u$ and $\bar{\Delta}_u$. Intuitively, a good $\hat{\Delta}_u \in \frac{1}{\beta}\mathcal{M}(\boldsymbol{B}_{\boldsymbol{\Delta}_u})$ (causing a small difference) is all-pass with $\bar{\sigma}(\hat{\Delta}_u) = \frac{1}{\beta}\ \forall\ \omega \in \Omega$ and with a perfect approximation of the phase data of $\bar{\Delta}_u$. In this respect, $\bar{\Delta}'_u$ with $\bar{\sigma}(\bar{\Delta}'_u) = \frac{1}{\beta}\ \forall\ \omega \in \Omega$ and $\arg(\bar{\Delta}'_u) = \arg(\bar{\Delta}_u)\ \forall\ \omega \in \Omega$ will be used as modified WCU data. Alternatively, a $\bar{\Delta}'_u$ with flat magnitude $\frac{1}{\beta}$ and newly generated phase data could be used. This new $\arg(\bar{\Delta}'_u)$ may be better suited for the case with restricted WCU magnitude. From the μ-definition (2.4) it is seen, that this involves a constrained optimization procedure ($\Delta \in \frac{1}{\beta}\boldsymbol{B}_{\boldsymbol{\Delta}_u}$ instead of $\Delta \in \boldsymbol{\Delta}$). This will not be considered and could be a subject for further research.

The WCU representation may be improved by a higher order of $\hat{\Delta}_u$. However, the order of $\tilde{G}$ equals the order of G plus the order of $\hat{\Delta}_u$ and increasing the order of $\hat{\Delta}_u$ may increase the computation time for IO selection. If the difference between $\bar{\sigma}(\mathcal{F}_u(M^\star, \hat{\Delta}_u))$ and $\bar{\sigma}(\mathcal{F}_u(M^\star, \bar{\Delta}'_u))$ is small, the order of $\hat{\Delta}_u$ may be qualified high enough. So, there is a trade-off between effectiveness (a high order $\hat{\Delta}_u$ may improve effectiveness) and efficiency (a low order $\hat{\Delta}_u$ may improve efficiency).

To illustrate the construction procedures, a feigned RP problem for the mechanical system in Fig. 4.1 is considered. The mass, spring, and damper parameters are set to one. Constant

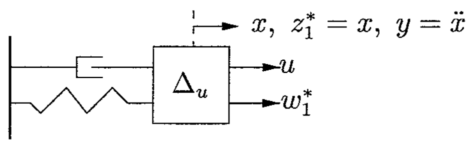

Figure 4.1: Mass-spring-damper example system

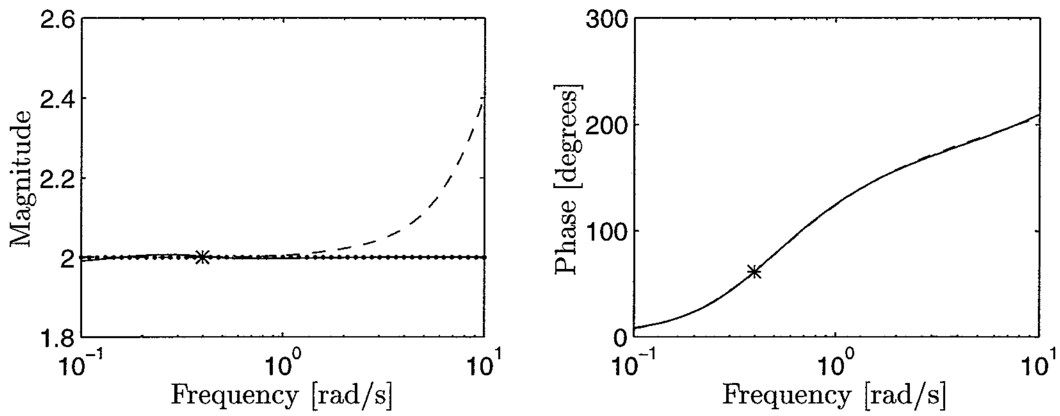

Figure 4.2: WCU data $\bar{\Delta}_u$ (- -), flattened magnitude data $|\bar{\Delta}'_u|$ (··), and fourth order unstable WCU representation $\hat{\Delta}_u$ (–); $*$ corresponds to ω_0 where μ is largest.

design filters are used: the filters for the regulated displacement z_1^* and the disturbance force w_1^* are set to 0.5 and the filters for the control force z_2^* and the acceleration sensor noise w_2^* are fixed at 0.1. The mass parameter is considered 100% uncertain. For a pure nominal performance problem (no Δ_u), an $\mathcal{H}_\infty$ optimization yields $\|M\|_\infty = 0.25$, while $\|M\|_\infty = 0.00$ for a pure robust stability problem (no Δ_p). An optimal μ-synthesis for the RP problem yields $\|M\|_\mu = \beta = 0.50$. For a frequency grid Ω containing 51 logarithmically evenly spaced points between 0.1 and 10 [rad/s], Fig. 4.2 depicts the corresponding WCU data $\bar{\Delta}_u$ and the flattened data $\bar{\Delta}'_u$ used for the construction of $\hat{\Delta}_u$. With the μ-Tools function `fitsys`, a fourth order $\hat{\Delta}_u$ can be generated, which closely matches the magnitude and phase of $\bar{\Delta}'_u$, see Fig. 4.2. However, this $\hat{\Delta}_u$ has three unstable poles and thus cannot be used for IO selection.

A "nice" (*i.e.*, low order, "smooth," bounded inbetween data points) approximation to the WCU data $\bar{\Delta}'_u$ may be easily constructed if it is allowed unstable. However, a nice and stable WCU representation may be difficult to find, or may not be possible at all if the WCU data better matches an unstable representation. To guarantee stability, the perfect phase or perfect magnitude approximation could be dropped, as done in Section 4.1 and 4.2 respectively. In Section 4.3, a construction is discussed which perfectly matches the magnitude and phase in the data points, but the resulting high order $\hat{\Delta}_u$ may have undesirable behavior inbetween those points. Finally, Section 4.4 summarizes some additional approaches to WCU constructions, which could not be used successfully for the example system and which have no good perspectives for IO selection purposes in general.

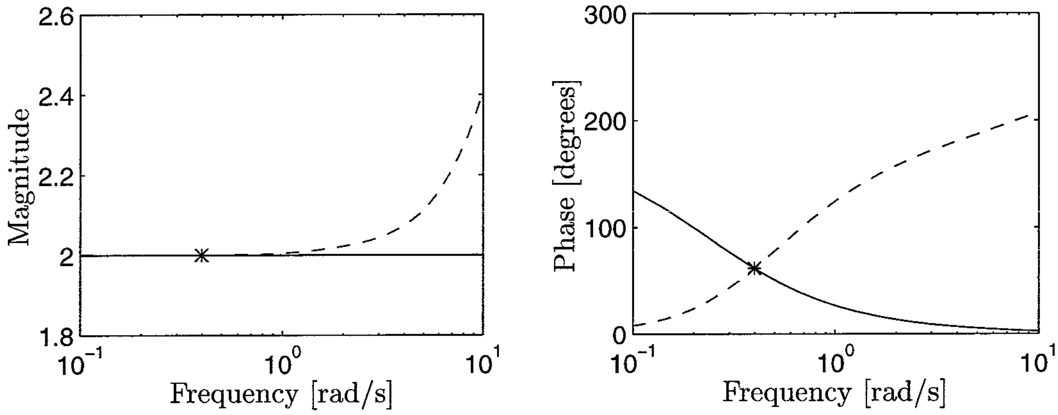

Figure 4.3: WCU data $\bar{\Delta}_u$ (- -) and all-pass, first order, and stable WCU representation $\hat{\Delta}_u$ (–); $*$ corresponds to ω_0 where μ is largest.

4.1 All-Pass WCU Representation

For the first construction, the function `dypert` from μ-Tools is used, see also [1, Chapter 4]. Assuming that Ω_0 consists of the single frequency ω_0, the resulting $\hat{\Delta}_u$ is perfect for ω_0. In the software, β in (3.2) corresponds to $\|M^*\|_{\mu_l}$, which is the lower bound version of $\|M^*\|_{\mu}$, see (2.21). For each $m_i \times n_i$ sub-block $\bar{\Delta}_{u_i}$, the WCU representation $\hat{\Delta}_{u_i}$ is all-pass with magnitude $\frac{1}{\beta}$ and order $m_i + n_i - 1$. For a scalar Δ_u, the `dypert` construction is easily interpreted. For the complex number $\bar{\Delta}_u(j\omega_0) = \bar{\Delta}_u'(j\omega_0)$ with $\omega_0 > 0$, there is a real number $\alpha > 0$ such that by a proper choice of the sign, the following holds:

$$\pm|\bar{\Delta}_u(j\omega_0)| \left.\frac{s-\alpha}{s+\alpha}\right|_{s=j\omega_0} = \bar{\Delta}_u(j\omega_0). \tag{4.1}$$

The WCU representation is then given by:

$$\hat{\Delta}_u = \pm|\bar{\Delta}_u(j\omega_0)| \frac{s-\alpha}{s+\alpha}. \tag{4.2}$$

If $\omega_0 = 0$ and $|\bar{\Delta}_u|$ is real and finite, all real $\alpha > 0$ are allowed; if $\omega_0 = 0$ and $|\bar{\Delta}_u|$ is complex or infinite, there is no solution. For a purely real number $\bar{\Delta}_u(j\omega_0)$ and $\omega_0 \geq 0$, $\alpha = 0$ and $\hat{\Delta}_u = \pm|\bar{\Delta}_u(j\omega_0)|$.

An advantage of the `dypert` representation is its relatively low order, leading to relatively small computation times for IO selection. A possible disadvantage is due to the `dypert` representation being based on WCU data for the single frequency ω_0. This fixes the behavior for all other frequencies in Ω and so the phase of $\bar{\Delta}_u(j\omega)$ and the phase of $\hat{\Delta}_u(j\omega)$ may differ significantly. For the example system, this is illustrated in Fig. 4.3, where $\omega_0 = 0.40$ [rad/s] and $\alpha = 0.24$ in (4.2).

4.2 Minimum-Phase WCU Representation

The second construction generates an $\mathcal{RH}_\infty$ WCU representation which closely matches the phase data of $\bar{\Delta}_u$. This construction is based on Bode's gain-phase relationship, see, *e.g*, [13, Section 2.1]. Consider a Single Input Single Output (SISO), stable, minimum-phase system $T(s)$ and assume $T(0) > 0$. The unique relation between the gain $|T(j\omega)|$ and the phase $\arg T(j\omega)$ [rad/s] of the frequency response is then given by:

$$\arg T(j\omega^*) = \frac{1}{\pi}\int_{-\infty}^{\infty} \underbrace{\frac{d\ln|T(j\omega)|}{d\ln\omega}}_{N(\omega)} \ln\left|\frac{\omega+\omega^*}{\omega-\omega^*}\right| \cdot \frac{d\omega}{\omega}. \tag{4.3}$$

The term $\ln\left|\frac{\omega+\omega^*}{\omega-\omega^*}\right|$ in (4.3) is infinite at $\omega = \omega^*$, so $\arg T(j\omega^*)$ is primarily determined by the local slope $N(\omega^*)$. Moreover, $\int_{-\infty}^{\infty} \ln\left|\frac{\omega+\omega^*}{\omega-\omega^*}\right| \cdot \frac{d\omega}{\omega} = \frac{\pi^2}{2}$, which justifies the following commonly used approximation for stable minimum-phase systems:

$$\arg T(j\omega^*) \approx \frac{\pi}{2}N(\omega^*) = \frac{\pi}{2}\frac{d\ln|T(j\omega^*)|}{d\ln\omega^*}. \tag{4.4}$$

In the context of IO selection, the approximation (4.4) is employed to generate new magnitude data for the WCU, based on the phase data $\arg\bar{\Delta}_u(j\omega)$. In a subsequent step, a minimum-phase $\mathcal{RH}_\infty$ representation $\hat{\Delta}_u$ is constructed for the combination of the original phase data and the new magnitude data, see below.

To generate new magnitude data, (4.4) is rewritten. Realizing that $d\ln\omega^* = \frac{1}{\omega^*}d\omega^*$, the following results:

$$\ln|T(j\omega)| \approx \frac{2}{\pi}\int_0^{\omega} \arg T(j\omega^*)\frac{1}{\omega^*}d\omega^* + c \quad\Leftrightarrow\quad |T(j\omega)| \approx Ce^{\frac{2}{\pi}\int_0^{\omega}\arg T(j\omega^*)\frac{1}{\omega^*}d\omega^*}, \tag{4.5}$$

with $C = e^c$ a constant to be chosen, see below. Given the phase $\arg\bar{\Delta}_u(j\omega)$, new magnitude data can be obtained by numerical integration over the frequency grid (in this report, a trapezoidal integration scheme is used). With the original phase data and the new magnitude data, the new WCU complex frequency response $\bar{\Delta}_u''$ is generated by substitution in:

$$\bar{\Delta}_u''(j\omega) = |\bar{\Delta}_u''(j\omega)|\, e^{j\arg\bar{\Delta}_u(j\omega)}. \tag{4.6}$$

Next, the μ-Toolbox function `fitsys` is used to generate a minimum-phase $\mathcal{RH}_\infty$ representation for $\bar{\Delta}_u''(j\omega)$. Finally, the constant C is used to scale the magnitude of this WCU representation so $\|\hat{\Delta}_u\|_\infty = \frac{1}{\beta}$.

For the example system, this construction is illustrated in Fig. 4.4. For an eighth order $\hat{\Delta}_u$, the phase is reasonably close to the phase of the data, while there is hardly any difference between $|\hat{\Delta}_u|$ and $|\bar{\Delta}_u''|$ (the latter is not depicted). The phase approximation cannot be further improved by increasing the order. This is due to the fact, that the `fitsys` function used for approximating $\bar{\Delta}_u''$ first generates an approximation which may have poles and zeros in the right half plane and then simply flips these poles and zeros around into the left half plane (for the eighth order $\hat{\Delta}_u$: three poles and two (out of eight) zeros in the right half

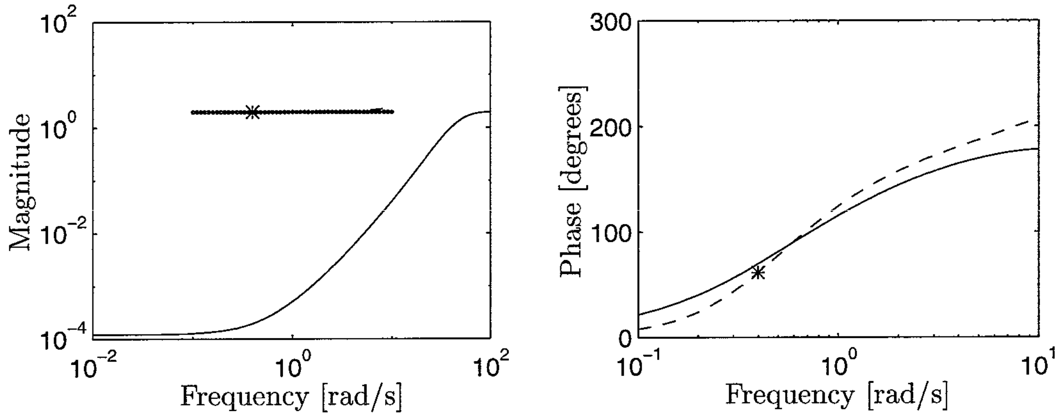

Figure 4.4: WCU data $\bar{\Delta}_u$ (--), flattened magnitude data $|\bar{\Delta}'_u|$ (··), and minimum-phase, eighth order, stable WCU representation $\hat{\Delta}_u$ (–); $*$ corresponds to ω_0 where μ is largest.

plane). While this leaves $|\hat{\Delta}_u|$ unchanged, this does not hold for $\arg \hat{\Delta}_u$. It is expected, that if the new data $\bar{\Delta}''_u$ exactly corresponds to a stable minimum-phase system, `fitsys` will also generate such a system. However, this ideal situation does not occur due to the approximation in (4.4). Note from Fig. 4.4, that $|\hat{\Delta}_u|$ is considerably smaller than $\frac{1}{\beta}$ in Ω; $\|\hat{\Delta}_u\|_\infty = \frac{1}{\beta}$ is achieved at $\omega = \infty$, *i.e.*, outside Ω.

4.3 Nevanlinna-Pick WCU Representation

The so-called Nevanlinna-Pick Interpolation (NPI) problem is considered to construct an $\mathcal{RH}_\infty$ WCU representation $\hat{\Delta}_u$ which *perfectly* matches the magnitude and phase of $\bar{\Delta}'_u$ for a *subset* of frequencies $\Omega_s \subseteq \Omega$. Only the "scalar" NPI problem is discussed here [3, Chapter 9], which yields a SISO transfer function $T(s)$. The more general "matrix" NPI problem can be found in [2, Chapter 18], or, as an alternative, the scalar NPI problem could be solved for each entry in $\bar{\Delta}'_u(j\omega)$.

Nevanlinna-Pick Interpolation Problem: Let $\{a_1, \ldots, a_n\}$ be a set of points in the right half-plane $\mathbb{C}^+$ and $\{b_1, \ldots, b_n\}$ a set of points in $\mathbb{C}$. The classical Nevanlinna-Pick interpolation problem is to find a complex-rational, proper, and stable transfer function $T(s)$ satisfying:

$$\|T\|_\infty \leq 1, \tag{4.7}$$

$$T(a_i) = b_i, \; i = 1, \ldots, n. \tag{4.8}$$

Equation (4.8) states that the graph of $T(s)$ must pass through each point (a_i, b_i). The NPI problem may not be solvable. A necessary condition for solvability is $|b_i| \leq 1 \; \forall \; i$. To guarantee solvability, the so-called Pick matrix (see [3, Section 9.2]) must be positive semi-definite. The ij-th entry of this matrix is given by $\frac{1-b_i b_j^*}{a_i + a_j^*}$. If the NPI problem is solvable, the algorithm documented in [3, Section 9.3] is used here to construct a solution. It is emphasized, that there are an infinite number of solutions if $|b_i| < 1$, because a complex-rational, proper, and stable transfer function $Q(s)$, $\|Q(s)\|_\infty \leq 1$ is free to choose. The effect of Q on $T(s, Q(s))$ is not easily interpreted and therefore $Q = 0$ or $Q = 1$ will be used here.

The interpolation of the data in $\bar{\Delta}'_u(j\omega)$ differs from the classical NPI problem in a few respects, but this does not cause insurmountable problems. First, the data points $a_i = j\omega_i$ are located on the imaginary axis instead of in $\mathbb{C}^+$. This boundary NPI problem is treated in [2, Chapter 21], where a "trick" for the discrete-time case gives rise to the following idea to retain the classical NPI problem. The data $a_i = j\omega_i$ is shifted into $\mathbb{C}^+$ by adding a small positive real number ϵ: $\tilde{a}_i = \epsilon + j\omega_i \ \forall\ i$. By choosing ϵ arbitrarily close to zero, it can be shown that the NPI problem for the shifted frequency data is always solvable if $|b_i| \leq 1$. However, to avoid numerical problems, ϵ should not be chosen too small in practice. After solving the NPI problem, the state-space matrix A of $T(s)$ is transformed into $A - \epsilon I$.

Second, the classical NPI problem aims at constructing a *complex*-rational transfer function, while $\hat{\Delta}_u$ must be *real*-rational. However, [3, Chapter 9] states the following: if the data in $\{a_1, \ldots, a_n\}$ and $\{b_1, \ldots, b_n\}$ occurs in complex conjugate pairs, then a complex-rational solution $T(s)$ can be written as $T(s) = \Re(T(s)) + j\Im(T(s))$ and the real-rational part $\Re(T(s))$ is also a solution to the NPI problem. Realizing that for a real-rational solution $T(s^*) = T^*(s)$, the frequency data vector and the WCU data vector are augmented with their complex conjugates to give $\begin{bmatrix} -j\omega \\ j\omega \end{bmatrix}$ and $\begin{bmatrix} \bar{\Delta}'^*_u(j\omega) \\ \bar{\Delta}'_u(j\omega) \end{bmatrix}$ respectively, which are supplied to the construction algorithm of [3, Section 9.2].

Third, for the classical NPI problem to be solvable each $|b_i|$ should not be larger than one. This will not hold in general and therefore, $\bar{\Delta}'_u(j\omega)$ is scaled as follows:

$$\bar{\Delta}''_u(j\omega) := \frac{\bar{\Delta}'_u(j\omega)}{\theta_1\theta_2}, \quad \text{with } \theta_1 := \max_{\omega_i}(|\bar{\Delta}'_u(j\omega_i)|) \tag{4.9}$$

and with θ_2 a positive real number slightly larger than one. From examples it is observed, that for $\theta_2 = 1$ the NPI problem may not be solvable if ϵ is not small enough. For the scaled data, the construction algorithm of [3, Section 9.3] is invoked and the solution is scaled backwards by multiplying with $\theta_1\theta_2$.

A more accurate WCU representation is obtained if Ω_s contains more frequency points, but this will increase the order of $\hat{\Delta}_u$. More specific, for N_s frequencies in Ω_s, the order of $\hat{\Delta}_u$ is $4N_s$. Recall, that the frequency data is mirrored into the real axis, so the construction is actually based on $2N_s$ data points. So, the order of $\hat{\Delta}_u$ grows rapidly with N_s, which endangers the IO selection efficiency.

In Fig. 4.5, the NPI construction procedure is illustrated for the mass-spring-damper system. Parameters $\epsilon = 10^{-4}$ and $\theta_2 = 1.01$ are used, $Q(s) = 0$, and Ω_s contains six logarithmically evenly spaced points in Ω (if more points are used, numerical problems occur). A 24th order WCU representation $\hat{\Delta}_u$ results. For this example, there is hardly any difference if $Q(s) = 1$ is used instead of $Q(s) = 0$. Figure 4.5 shows, that $\hat{\Delta}_u$ exactly equals $\bar{\Delta}'_u$ in the data points. However, inbetween these points there are large differences between the data and the approximation, especially for the phase (note, that the phase plot is now restricted to the range $[-180°, 180°]$). Indeed, the NPI problem does not impose other requirements inbetween data points than the $\mathcal{H}_\infty$ norm requirement on $T(s)$.

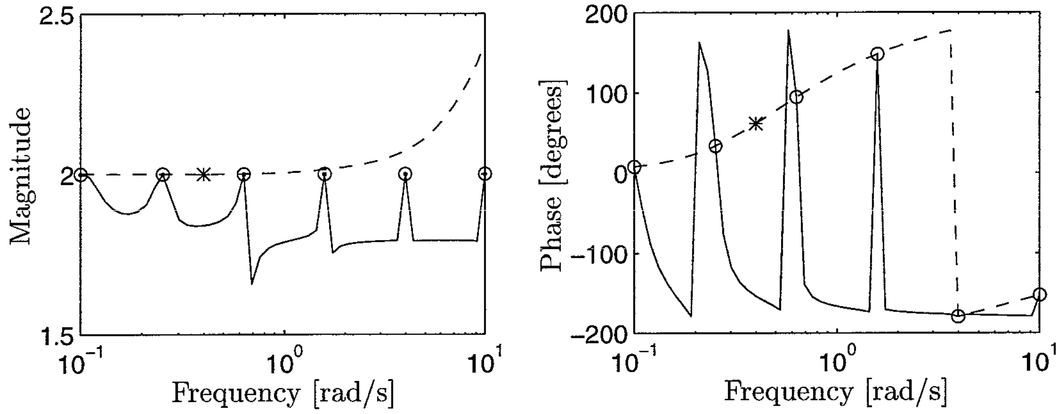

Figure 4.5: WCU data $\bar{\Delta}_u$ (- -), flattened WCU data $|\bar{\Delta}'_u|$ for Ω_s (o), and 24th order stable WCU representation $\hat{\Delta}_u$ (–) based on Nevanlinna-Pick interpolation; $*$ corresponds to ω_0 where μ is largest.

4.4 Other WCU Constructions

The findings with some other construction procedures are summarized. Since they were not successful for the mass-spring-damper example and are expected not to be useful in general, these procedures are not further considered for the IO selection application in Chapter 5.

The first construction amounts to approximating an unstable transfer function by a stable one. As shown for the example, an unstable WCU representation with $\hat{\Delta}_u \approx \bar{\Delta}'_u$ may be easily constructed. The idea is now to split up the unstable $\hat{\Delta}_u$ into a stable part $\hat{\Delta}_u^+ \in \mathcal{RH}_\infty$ and an anti-stable part $\hat{\Delta}_u^- \in \mathcal{RH}_\infty^-$ (all poles in the right half plane), so $\hat{\Delta}_u = \hat{\Delta}_u^+ + \hat{\Delta}_u^-$. Next, the anti-stable part is replaced by a stable transfer function, which results from solving the so-called Nehari problem, see, *e.g.*, [21, Chapter 8] and [9, Section 6.6]. Essentially, a minimization problem in the form $\inf_{S\in\mathcal{RH}_\infty} \|R-S\|_\infty$ is solved, with $R \in \mathcal{RH}_\infty^-$. Afterwards, the stable approximation of the anti-stable $\hat{\Delta}_u^-$ is added to the stable part $\hat{\Delta}_u^+$ to give a stable WCU representation. Since the Nehari problem only involves an $\mathcal{H}_\infty$ norm minimization related to the anti-stable part, the resulting $\hat{\Delta}_u$ may differ considerably from the original data $\bar{\Delta}'_u$. This has also been observed for the mass-spring-damper example; see Fig. 4.6, where the third order anti-stable part of the unstable $\hat{\Delta}_u$ in Fig. 4.2 is replaced by a second order stable transfer function.

The second type of constructions *a priori* require the poles of $\hat{\Delta}_u$ to have a negative real part (via constraints in the involved optimizations). In [6], an approach is described that in the SISO case aims at finding a stable transfer function $\hat{\Delta}_u(s)$ that optimally describes the frequency-response data $\bar{\Delta}'_u(j\omega)$ in a weighted l_∞-sense ("minimize the maximum magnitude of the weighted error"). The construction involves two steps: first, an initial estimate for $\hat{\Delta}_u$ is generated by *linear* programming; second, this estimate is improved by solving a *nonlinear* programming approach. The first step is implemented in the MATLAB compatible package CURVEFIT [5], but the second step is not. However, according to [5], in many cases the optimal approximation after the second step is hardly any better than the initial estimate.

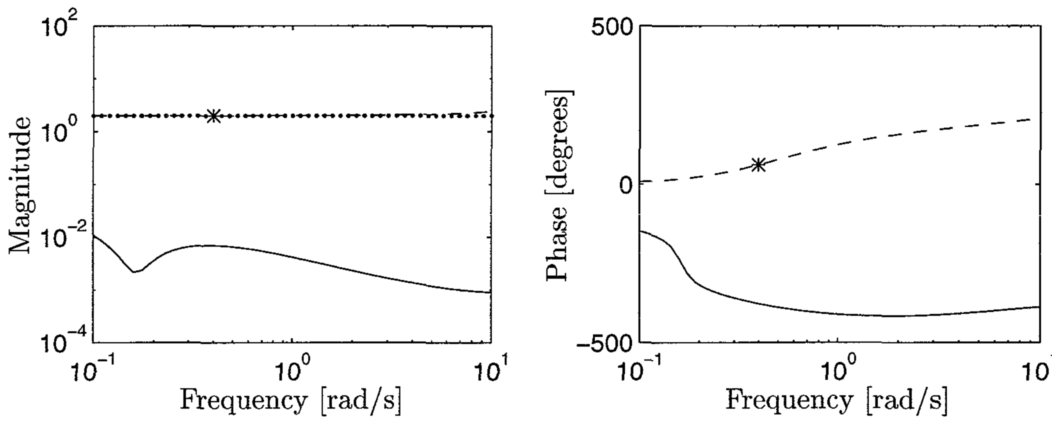

Figure 4.6: WCU data $\bar{\Delta}_u$ (- -), flattened WCU data $|\bar{\Delta}_u'|$ (··), and third order stable WCU representation $\hat{\Delta}_u$ (–) from solving the Nehari problem; $*$ corresponds to ω_0 where μ is largest.

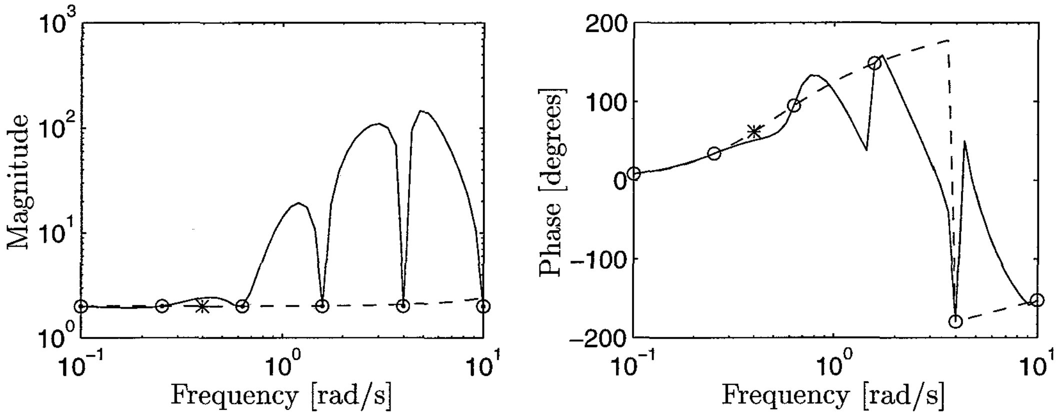

Figure 4.7: WCU data $\bar{\Delta}_u$ (- -), flattened WCU data $|\bar{\Delta}_u'|$ for Ω_s (o), and 12th order stable WCU representation $\hat{\Delta}_u$ (–) from CURVEFIT; $*$ corresponds to ω_0 where μ is largest.

To get an idea of the prospects of this construction, the first step is solved for the example.

Up to our knowledge, there are two MATLAB functions to construct stable transfer functions. First, `fitsys` from μ-Tools could be used, but the algorithm is not documented. Second, `invfreqs` from the Signal Processing Toolbox [7] involves a weighted minimization in l_2-sense ("minimize the sum of the weighted squared errors").

Using any of these three construction procedures for the example system, it is observed that the approximation inbetween data points may be arbitrarily bad, both with respect to magnitude and phase. This is due to the fact that only a finite number of data points is considered and the construction procedures do not impose requirements inbetween points (this is unknown for the `fitsys` algorithm). While the Nevanlinna-Pick procedure guarantees an $\mathcal{H}_\infty$ norm bound for $\hat{\Delta}_u$, this does not apply for these procedures. For the CURVEFIT procedure, the above is illustrated in Fig. 4.7. Also, the procedures easily run into numerical problems, even for a small number of frequency points in the subset Ω_s of Ω.

Chapter 5

IO Selection for an Active Suspension

The IO selection method is used to select actuators and sensors for active vehicle suspension control. Section 5.1 sketches this problem. For nine typical IO sets, controllers are designed and the results of $\mathcal{H}_\infty$ optimizations for differently perturbed plants are compared in Section 5.2. Finally, Section 5.3 discusses the IO selection results for 45 candidate IO sets and compares the efficiency and effectiveness of the proposed method with those of two other methods.

5.1 Control Problem Formulation

An active suspension for the tractor-semitrailer combination in Fig. 5.1 is considered. To control the suspension, two actuators (u_1, u_2) placed between the axles and the tractor chassis are proposed as candidate inputs, while suspension deflection sensors (y_1, y_2) and chassis acceleration sensors (y_3, y_4) are suggested as candidate outputs. This yields 45 distinct candidate IO sets.

The control objectives are the following. First, the heave (z_1^*) and pitch (z_2^*) accelerations should be small for good driver comfort. Second, the suspension deflections (z_3^*, z_4^*) must satisfy space limitations and, third, the tire deflections (z_5^*, z_6^*) must be limited for good handling properties and minimum road surface damage. Finally, z^* contains weights for each input u to account for actuator limitations. The exogenous variables w^* are the derivatives of the road surface height (w_1^*, w_2^*) and the noise for each output y. The design filters in the generalized plant G quantifying these control objectives are documented in [15, 18] and not repeated here.

Due to cargo variations, the semitrailer mass is a major uncertainty source; see the point mass "Δ_u" in Fig. 5.1. This mass is assumed to vary between the values for an empty and fully

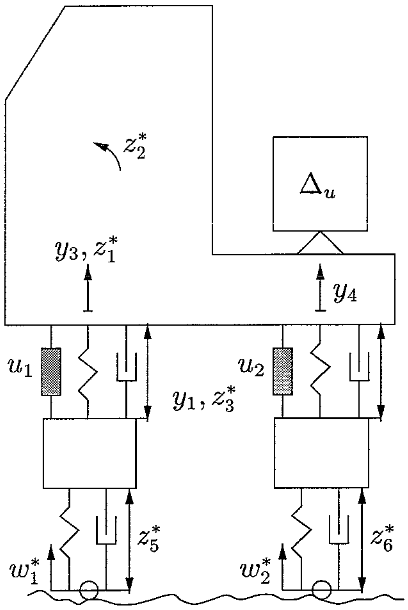

Figure 5.1: Tractor-semitrailer combination

loaded semitrailer, with the nominal mass taken the mean of these two. This gives a 90% variation around the nominal value. Note, that Δ_u is real parametric. However, the IO selection method and controller designs in this report assume complex uncertainties and may therefore yield conservative results. Since Δ_u has dimension 1×1, the WCU representation $\hat{\Delta}_u$ is found by constructing a scalar transfer function.

Figure 5.2 depicts the μ-plot (dashed) after an optimal μ-synthesis for the full IO set. The plot is relatively flat for frequencies below 100 [rad/s] and the maximum value $\|M^\star\|_\mu = \|M^\star\|_{\mu_l} = \beta = 0.75$ is reached around $\omega_0 = 33$ [rad/s]. The magnitude and phase of the corresponding WCU data is shown in Fig. 5.3 (and Fig. 5.4). For this problem, only an *unstable* WCU representation $\hat{\Delta}_u$ could be generated which closely matches the modified WCU data $\bar{\Delta}'_u$. Therefore, the two WCU constructions proposed in Section 4.1 and 4.2 are invoked. The construction based on Nevanlinna-Pick interpolation is not considered, since it causes numerical problems if more than one data point is supplied to the algorithm. These problems are due to approximate pole/zero cancellations in $\hat{\Delta}_u$ and they may also be due to the poles and zeros being close to the imaginary axis.

The all-pass and minimum-phase WCU representations are depicted in Fig. 5.3 and 5.4 respectively and the magnitudes of the closed-loops with $\hat{\Delta}_u$ absorbed are shown in Fig. 5.2. The first order all-pass $\hat{\Delta}_u$ is perfect (in magnitude and phase) for $\omega = \omega_0$, but for other frequencies it deviates significantly from the data. If $\hat{\Delta}_u$ is absorbed into $M^\star$, Fig. 5.2 shows that $\bar{\sigma}(\mathcal{F}_u(M^\star, \hat{\Delta}_u)) = \bar{\sigma}(\mathcal{F}_u(M^\star, \bar{\Delta}_u))$ for $\omega = \omega_0$. For other frequencies, $\bar{\sigma}(\mathcal{F}_u(M, \hat{\Delta}_u)) \leq \bar{\sigma}(\mathcal{F}_u(M^\star, \bar{\Delta}_u))$. Obviously, $\hat{\Delta}_u$ is not worst case $\forall\ \omega \in \Omega$. For the minimum-phase $\hat{\Delta}_u$, the phase approximation cannot be improved by increasing the order further than six. Though $\arg \hat{\Delta}_u$ fits reasonably well with $\arg \bar{\Delta}_u$, the magnitude $|\hat{\Delta}_u|$ is considerably smaller than $|\bar{\Delta}'_u|$. The all-pass and minimum-phase WCU representations both meet the three assumptions listed in Section 2.3.

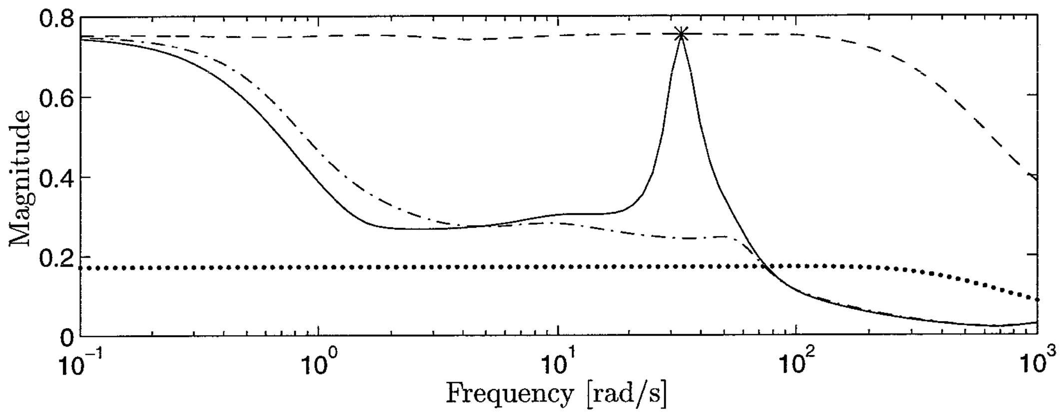

Figure 5.2: Magnitude of the perturbed TFM between w^* and z^* for the WCU data $\bar{\sigma}(\mathcal{F}_u(M^\star, \bar{\Delta}_u)) = \mu_{\mathbf{\Delta}}(M^\star)$ (- -), for the minimum-phase WCU representation $\bar{\sigma}(\mathcal{F}_u(M^\star, \hat{\Delta}_u))$ (—·), and for the all-pass WCU representation before (–) and after (··) $\mathcal{H}_\infty$ optimization; $*$ corresponds to (ω_0, β)

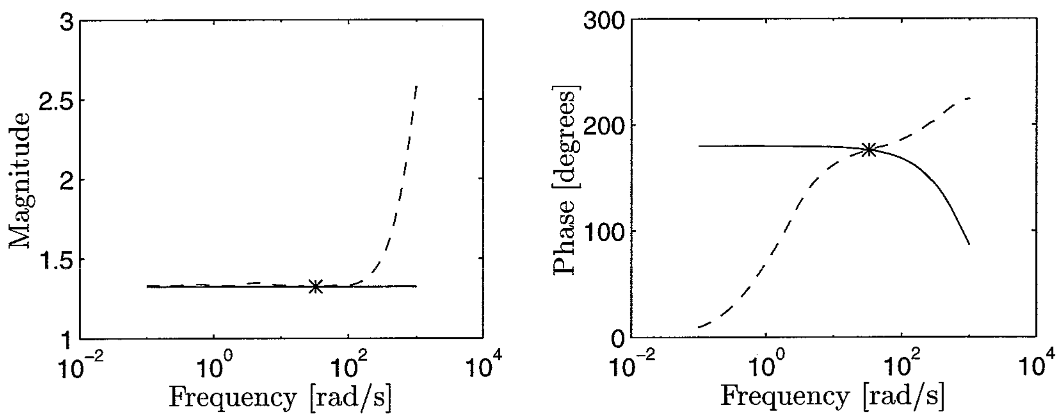

Figure 5.3: Worst case uncertainty data $\bar{\Delta}_u$ (- -) for the full IO set and first order all-pass WCU representation $\hat{\Delta}_u$ (–); $*$ corresponds to (ω_0, β)

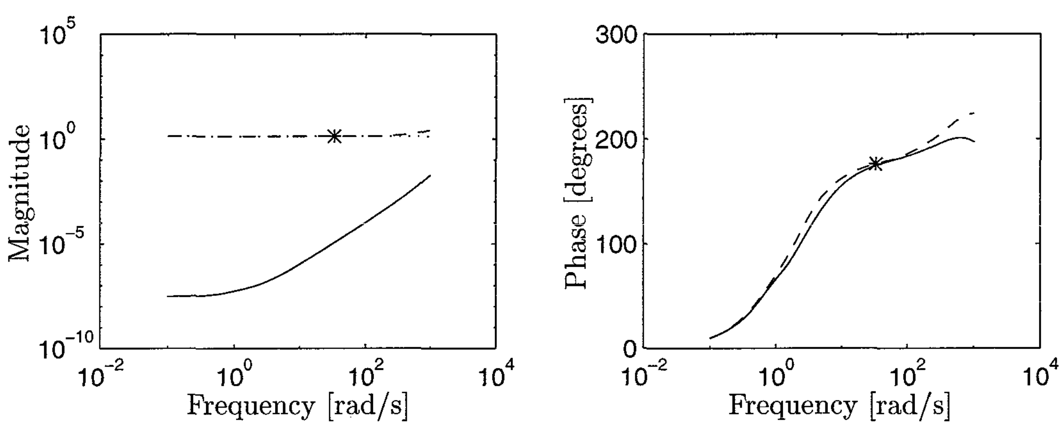

Figure 5.4: Worst case uncertainty data $\bar{\Delta}_u$ (--) for the full IO set, flattened magnitude data $|\bar{\Delta}'_u|$ ($\cdot\cdot$), and sixth order minimum-phase WCU representation $\hat{\Delta}_u$ (–); $*$ corresponds to (ω_0, β)

5.2 $\mathcal{H}_\infty$ Optimizations for Perturbed Plants

Prior to the IO selection in Section 5.3, $\mathcal{H}_\infty$ optimizations are performed for generalized plants absorbing $\hat{\Delta}_u$'s with distinct magnitudes ($\min_{K\in\mathcal{K}_A} \|\mathcal{F}_l(\tilde{G},K)\|_\infty$, with $\texttt{tol}=10^{-3}$ in the γ-iteration). This will be done for the nine IO sets in Table 5.1, which give a good indication of the importance of each candidate actuator and sensor. Based on the $\|M\|_\mu$ values from optimal μ-synthesis, it is concluded that the actuator (u_2) and sensors (y_2 and y_4) at the rear of the tractor are more important for RP than those at the front. Table 5.1 also lists the optimal $\|M\|_\infty$ values for Nominal Performance (NP), *i.e.*, for the case without uncertainty. Recall, that $\tilde{\Delta}_u = \frac{\beta}{\gamma}\hat{\Delta}_u \in \frac{1}{\gamma}\mathcal{M}(\boldsymbol{B}_{\boldsymbol{\Delta}_u})$. So, by manipulating γ, the magnitude of the WCU representation is varied. For the all-pass $\tilde{\Delta}_u$, three different cases are considered: 1) $\gamma = 1$, 2) $\gamma = 0.8$, and 3) $\gamma = \beta = 0.75$. For the minimum-phase $\tilde{\Delta}_u$, only $\gamma = 1$ and $\gamma = \beta$ are studied.

Applying the *minimum-phase* WCU representation $\tilde{\Delta}_u$, Table 5.1 shows that $\|\tilde{M}\|_\infty$ is the same for $\gamma = 1$ and for $\gamma = \beta$. Moreover, $\|\tilde{M}\|_\infty = \|M\|_\infty$, *i.e.*, the smallest achievable closed-loop $\mathcal{H}_\infty$ norm is the same for the generalized plant with $\tilde{\Delta}_u$ absorbed and for the generalized plant without uncertainty ("$\tilde{\Delta}_u = 0$"). Apparently, $\tilde{\Delta}_u$ is too small, as may have been foreseen from Fig. 5.4. For this reason, the minimum-phase WCU representation is not further considered in this chapter.

The *all-pass* WCU representation $\tilde{\Delta}_u$ is now studied. A first observation from Table 5.1 is, that for the full IO set absorbing $\hat{\Delta}_u$ ($= \tilde{\Delta}_u$ for $\gamma = \beta$) into G yields $\|\tilde{M}\|_\infty = 0.17$, which is significantly smaller than $\|M\|_\mu = 0.75$. This is because $\hat{\Delta}_u$ is not the worst case uncertainty $\forall\ \omega \in \Omega$, not even for the full IO set (see Fig. 5.2). As a result, the new controller from an $\mathcal{H}_\infty$ optimization for $\tilde{G}$ can further reduce $\bar{\sigma}(\mathcal{F}_u(M^\star, \hat{\Delta}_u))$ for frequencies where this magnitude is large (*e.g.*, for $\omega = \omega_0$), by letting it increase for frequencies where it is small. Figure 5.2 illustrates this effect. $\mathcal{H}_\infty$ optimization for $\tilde{G}$ returns a closed-loop magnitude which is considerably smaller than $\bar{\sigma}(\mathcal{F}_u(M^\star, \hat{\Delta}_u))$ for frequencies below 76 [rad/s], yielding

Table 5.1: Nine typical IO sets with $\|M\|_\mu$ from optimal μ-syntheses (RP), $\|M\|_\infty$ from $\mathcal{H}_\infty$ optimizations without uncertainty (NP), and with $\|\tilde{M}\|_\infty$ from $\mathcal{H}_\infty$ optimizations with $\tilde{\Delta}_u$ absorbed into G.

IO set	outputs	inputs	$\|M\|_\mu$ (RP)	$\|M\|_\infty$ (NP)	$\|\tilde{M}\|_\infty$, all-pass $\gamma=1$	$\gamma=0.8$	$\gamma=\beta$	$\|\tilde{M}\|_\infty$, min-phase $\gamma=1$	$\gamma=\beta$
1	$y_1\,y_2\,y_3\,y_4$	$u_1\,u_2$	0.75	0.15	0.15	0.15	0.17	0.15	0.15
2	$y_1\,y_2\,y_3\,y_4$	u_1	1.06	0.17	0.23	16.35	11.64	0.17	0.17
3	$y_1\,y_2\,y_3\,y_4$	u_2	0.75	0.27	0.28	0.27	0.27	0.27	0.27
4	$y_1\,y_2$	$u_1\,u_2$	0.76	0.15	0.15	0.19	0.25	0.15	0.15
5	$y_3\,y_4$	$u_1\,u_2$	0.76	0.16	0.15	0.16	0.17	0.16	0.16
6	y_1	$u_1\,u_2$	1.01	0.16	0.23	12.54	13.93	0.16	0.16
7	y_2	$u_1\,u_2$	0.76	0.27	0.28	0.26	0.26	0.27	0.27
8	y_3	$u_1\,u_2$	0.83	0.17	0.22	0.51	0.53	0.17	0.17
9	y_4	$u_1\,u_2$	0.76	0.28	0.28	0.27	0.27	0.28	0.28

a too optimistic indication $\|\tilde{M}\|_\infty$ of the achievable RP level.

A second observation from Table 5.1 is, that each $\|\tilde{M}\|_\infty$ for $\gamma = 1$ is considerably smaller than one for all typical IO sets, even for IO sets 2 and 6 with $\|M\|_\mu > 1$. So, the nine IO sets pass the necessary condition for existence of a controller achieving the RP level $\gamma = 1$. Moreover, each $\|\tilde{M}\|_\infty$ is significantly smaller than the corresponding $\|M\|_\mu$. Apparently, the applied WCU representation is much "smaller" than the true WCU for each IO set. Also notice, that a smaller $\|\tilde{M}\|_\infty$ does not imply a smaller $\|M\|_\mu$; compare, *e.g.*, IO set 2 and 3. Therefore, predicting the IO sets' lowest achievable $\|M\|_\mu$ based on $\|\tilde{M}\|_\infty$ seems useless if $\tilde{\Delta}_u$ is not representative. For the smaller value $\gamma = 0.8$ (and hence for larger $\tilde{\Delta}_u$), IO sets 2 and 6 yield $\|\tilde{M}\|_\infty > 0.8$, which is in line with their $\|M\|_\mu$ values. For IO set 8, however, $\|\tilde{M}\|_\infty < 0.8$ despite the fact that $\|M\|_\mu > 0.8$.

Next, the focus is on $\gamma = \beta$, which is the case without down-scaling: $\tilde{\Delta}_u = \hat{\Delta}_u$. Under the assumption that the μ-synthesis results are correct, $\|M\|_\mu < 0.75$ is only possible for typical IO sets 1 and 3. All nine $\|\tilde{M}\|_\infty$ values are smaller than the corresponding $\|M\|_\mu$ values, except for IO sets 2 and 6. For these IO sets, $\|\tilde{M}\|_\infty > 0.75$ and so they are correctly rejected for $\gamma = 0.75$. However, IO set 8 is incorrectly accepted. These results are made plausible by Fig. 5.5, which shows that for IO sets 2 and 6 the magnitude of $\hat{\Delta}_u$ is considerably larger than that of the actual WCU data $\bar{\Delta}_u$ for frequencies in a region around ω_0 (mind the different y-axis ranges and assess the results for IO sets 4, 7, and 8 in this perspective). For IO sets 2 and 6, the maximum of μ and hence the minimum of $\bar{\sigma}(\bar{\Delta}_u)$ also occurs at a different frequency $\omega_0 \approx 13$ [rad/s] than for the full IO set.

Table 5.1 also shows, that for IO sets 5, 7, and 9 the optimal $\|M\|_\infty$ value for NP may be slightly larger than the optimal $\|\tilde{M}\|_\infty$ value with $\tilde{\Delta}_u$ absorbed into the nominal generalized

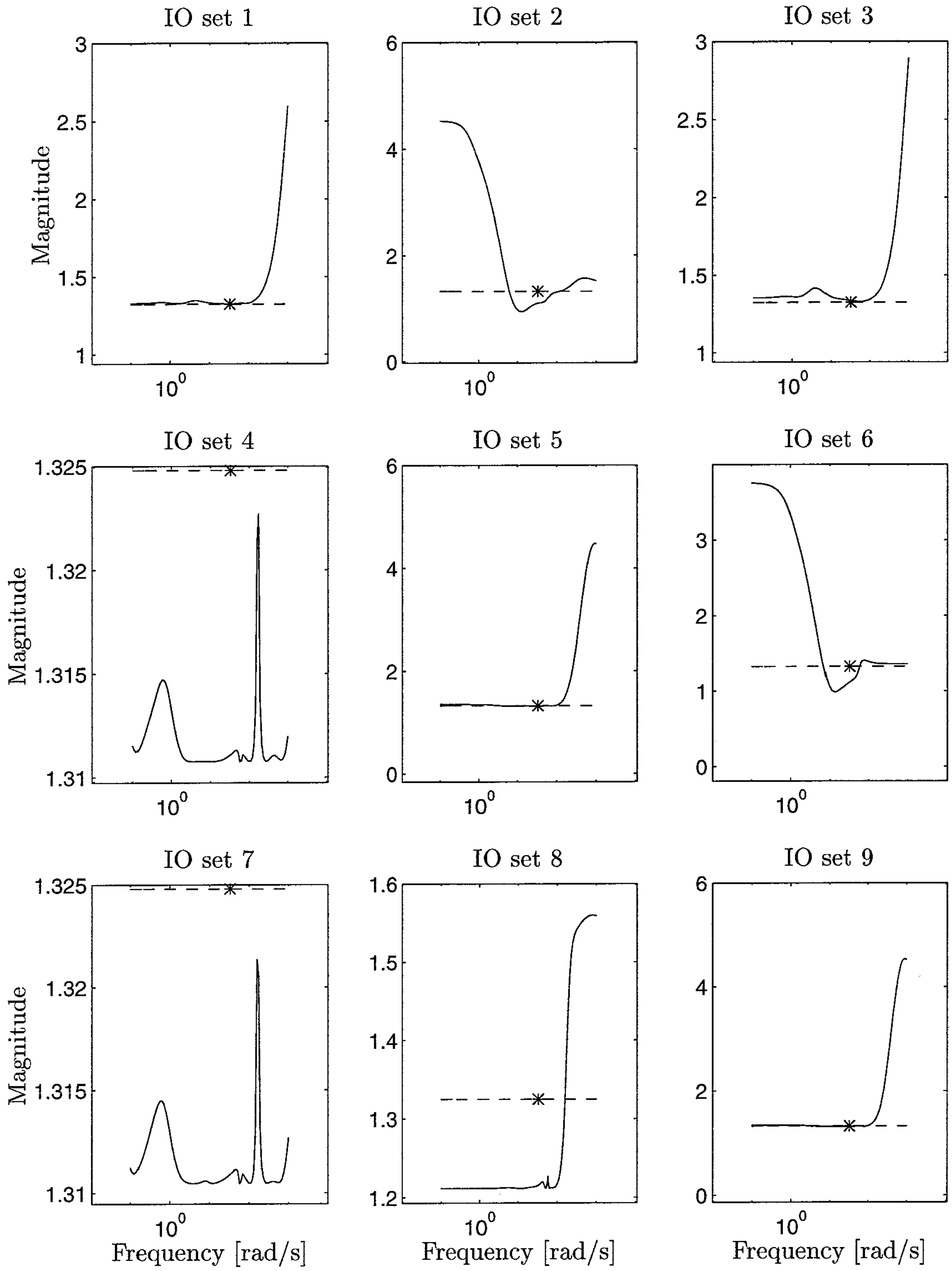

Figure 5.5: Magnitude of the WCU data $\bar{\Delta}_u$ for each of the typical IO sets' optimal closed-loops (–) and magnitude of the all-pass WCU representation $\hat{\Delta}_u$ (- -) for the *full* IO set's optimal closed-loop; $*$ is located at ($\omega_0 = 33, \frac{1}{\beta} = \frac{1}{0.75}$)

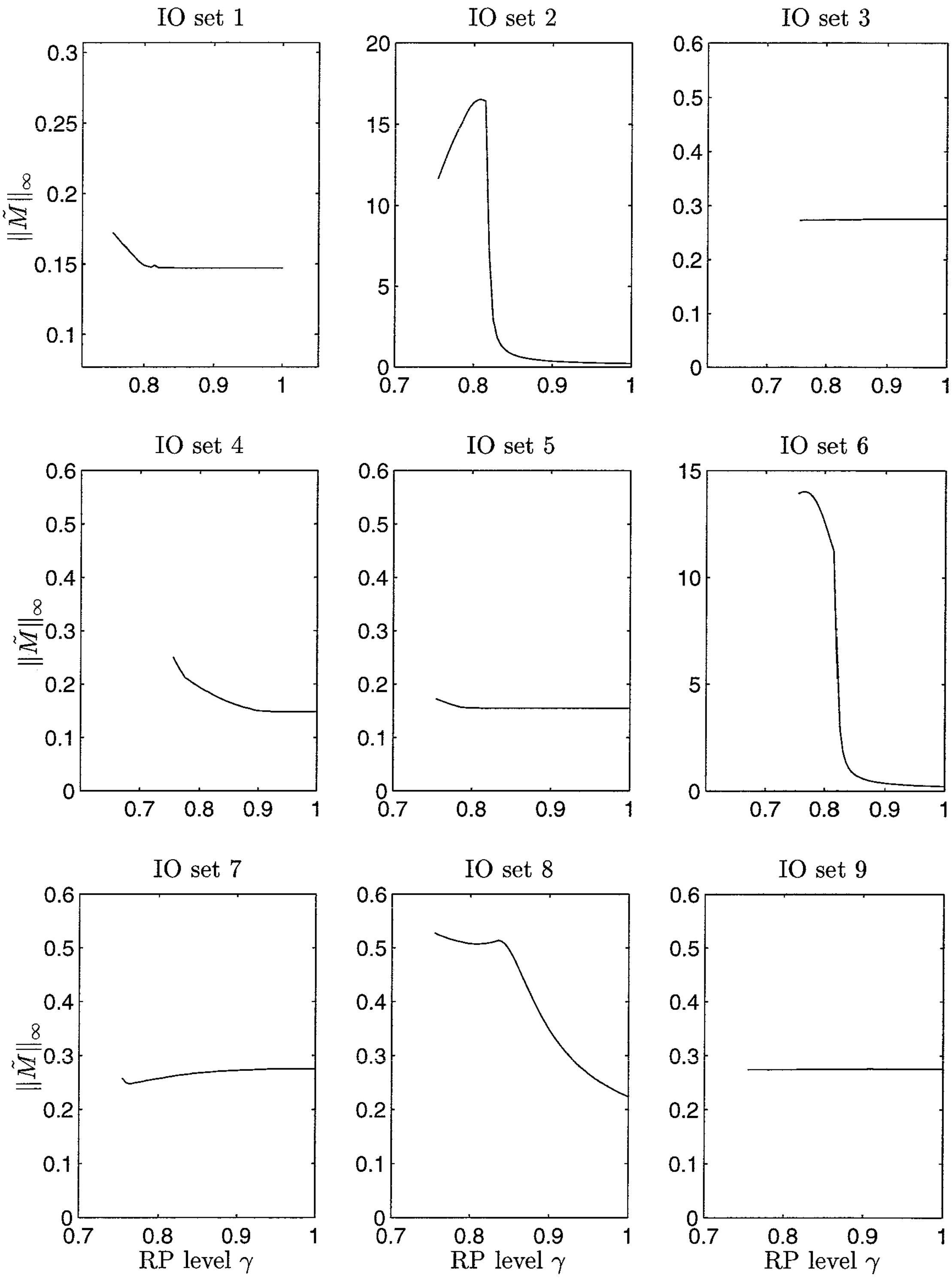

Figure 5.6: $\|\tilde{M}\|_\infty$ as a function of the RP test level γ for the nine typical IO sets in Table 5.1

plant. Moreover, for IO sets 3, 7, and 9 the optimal $\|\tilde{M}\|_\infty$ may slightly decrease for an increasing magnitude of $\tilde{\Delta}_u$; for IO set 2, the decrease is large if $\gamma = \beta$ is used instead of $\gamma = 0.8$. An exact explanation for these counter-intuitive phenomena ("performance is better in case of (a larger) uncertainty") is currently lacking. Apparently, if the WCU representation is not worst case $\forall\ \omega \in \Omega$, absorbing it into the plant may have a positive effect on the plant dynamics. For the nine typical IO sets, the effect of varying γ in the range [0.75, 1] on the optimal $\|\tilde{M}\|_\infty$ is shown graphically in Fig. 5.6. Quite counter-intuitively, $\|\tilde{M}\|_\infty$ for IO sets 2, 6, 7, and 8 does not monotonically decrease for increasing γ and hence decreasing magnitude of $\tilde{\Delta}_u \in \frac{1}{\gamma}\mathcal{M}(\boldsymbol{B}_{\boldsymbol{\Delta}_u})$.

5.3 Input Output Selection Results

IO selection is performed for the 45 candidate IO sets. The results of the proposed method involving the WCU representation (*WCU-based IO selection*) are compared with the results from two other approaches:

1. *μ-based IO selection:* This method is based on the *D-K* iteration approach to suboptimal μ-synthesis, see, *e.g.*, [21, Chapter 11]. Using third order *D*-scales and a frequency grid with 60 points between 10^{-1} and 10^3 [rad/s], the *D-K* iteration is stopped in two cases: if $\|M\|_\mu < \gamma$ (IO set is viable), or if the reduction in $\|M\|_\mu$ is less than 0.01 and $\|M\|_\mu > \gamma$ (IO set is nonviable). One of these criteria is usually met within five iteration steps. Assuming the μ-synthesis results to be correct, this method provides a *necessary and sufficient* condition for IO set viability.

2. *DSE-based IO selection [15, 18]:* This method extends the generalized plants G with diagonal scalings. These are the so-called *D*-Scale Estimates (DSEs) obtained from a μ-analysis for the full IO set's optimal closed-loop $M^\star$. Since the DSE from the full IO set may not be optimal for other IO sets, this method provides a *sufficient* condition for IO set viability. Here, a fourth order DSE is used.

Starting with the full IO set, smaller candidates are checked and subsets of nonviable IO sets are directly rejected, since eliminating actuators and sensors will never improve control. Other suggestions to improve the efficiency are given in [15, Chapter 7]). The results of the three IO selection methods with different RP test levels γ are listed in Table 5.2. The CPU times apply for a Silicon Graphics workstation (Indy, 200MHz, R4400SC). It is emphasized, that for the WCU-based and DSE-based methods the CPU times *exclude* the time for optimal μ-synthesis with the full IO set (CPU=196 [s]). This is fair, because also for the μ-based IO selection, it is sensible to find out what the best achievable RP level is by first performing an optimal μ-synthesis for the full IO set.

The main conclusions from Table 5.2 are the following. For $\gamma = 1$, the μ-based IO selection rejects 17 IO sets. These are the 15 IO sets using the single front actuator u_1 and $y_1/u_1\,u_2$, y_1/u_2 with the single front suspension deflection sensor y_1. The WCU-based IO selection

Table 5.2: Number of accepted IO sets and CPU time for IO selection based on three different approaches

RP test level	μ-based		WCU-based		DSE-based	
	accepted sets	CPU [s]	accepted sets	CPU [s]	accepted sets	CPU [s]
$\gamma = 1$	28	$3.29\,10^3$	45	62	26	76
$\gamma = 0.8$	26	$3.81\,10^3$	28	42	24	67

method accepts all 45 IO sets, so 17 sets are incorrectly accepted. Note, that this ineffectiveness is in line with the $\mathcal{H}_\infty$ optimization results in Table 5.1. For $\gamma = 1$, the DSE-based IO selection rejects 19 IO sets, but $y_3/u_1\,u_2$ and y_3/u_2 can achieve $\|M\|_\mu = 0.83$ and so they are incorrectly rejected.

For $\gamma = 0.8$, 26 IO sets should be termed viable: in addition to the 17 IO sets nonviable for $\gamma = 1$, $y_3/u_1\,u_2$ and y_3/u_2 using the single front acceleration sensor y_3 should be eliminated. It appears, that the WCU based IO selection incorrectly accepts these two IO sets, while the DSE based method incorrectly eliminates $y_1\,y_3/u_1\,u_2$ and $y_1\,y_3/u_2$ with $\|M\|_\mu = 0.76$.

These results clearly show, that (due to necessity) the WCU-based method may incorrectly accept nonviable IO sets, while (due to sufficiency) the DSE-based method may incorrectly reject viable IO sets. Hence, both methods may not be effective, depending on the considered problem. Combining these two methods with μ-synthesis may improve effectiveness as follows. First, the candidate IO sets are subjected to the WCU-based method. Second, the accepted candidates are subjected to the DSE-based method. Obviously, the remaining IO sets are viable. However, for the IO sets accepted in the first step and rejected in the second step, it is unclear whether they are viable or not. For a manageable number of such IO sets, μ-synthesis could now be invoked to get an unambiguous answer to IO set viability. For the considered problem and $\gamma = 0.8$, four IO sets are accepted in the first step and rejected in the second step. These are the viable IO sets $y_1\,y_3/u_1u_2$ and $y_1\,y_3/u_2$ and the nonviable IO sets $y_3/u_1\,u_2$ and y_3/u_2.

Table 5.2 finally shows, that for this particular problem the WCU-based IO selection method is slightly more efficient than the DSE-based method. Though a larger number of IO sets are tested for the WCU-based method, the CPU times are smaller: a factor 1.2 and 1.6 for $\gamma = 1$ and $\gamma = 0.8$ respectively. This is due to the fact, that the DSEs increase the order of the generalized plant G by eight, while the WCU representation increases the order only by one. The DSE-based IO selection in turn is considerably more efficient than the μ-based IO selection: a factor 43 and 57 faster for $\gamma = 1$ and $\gamma = 0.8$ respectively.

Chapter 6

Discussion

A new method for actuator and sensor selection (IO selection) was proposed. Basically, the method eliminates the structure in the combined uncertainty/performance block arising in robust performance problems. This is achieved by constructing a real-rational, proper, and stable ($\mathcal{RH}_\infty$) representation of a Worst Case Uncertainty (WCU) and absorbing this into the generalized plant. For the remaining unstructured performance block, the IO selection method proposed in [14, 17] can be used. Essentially, the existence of a stabilizing controller achieving a closed-loop $\mathcal{H}_\infty$ norm bound is checked. This involves conditions on the solutions to two Riccati equations. The WCU data and $\mathcal{RH}_\infty$ WCU representation $\hat{\Delta}_u$ are determined from the full IO set's closed-loop after an optimal μ-synthesis. The IO selection relies on a necessary condition for IO set viability, since the WCU representation is not guaranteed to be really worst case for all frequencies, not even for the full IO set on which it is based.

A major problem encountered for the IO selection method is the requirement that $\hat{\Delta}_u$ must be stable. As a result, a suitable (close to data points, bounded inbetween data points, low order, "smooth") $\hat{\Delta}_u$ is not easily constructed and may not be possible at all. In this respect, a remaining question is if a simple criterion exists (or can be developed), which checks whether or not such a suitable WCU representation exists. Moreover, the way in which the WCU data is generated by the μ-Tools function `mu` could be studied more thoroughly, to find out if differently generated WCU data makes the construction of a stable $\hat{\Delta}_u$ possible. For the WCU data obtained with `mu`, the magnitude is flattened, while the phase is kept the same. This modified WCU data is used for the construction of $\hat{\Delta}_u$. As an alternative, a method could be developed to directly construct WCU data with all-pass magnitude. However, even if $\hat{\Delta}_u$ perfectly matches the WCU data for the full IO set, it may not be the worst case for other IO sets. So, another remaining question is, if the effectiveness can be predicted of IO selection with $\hat{\Delta}_u$ derived for the full IO set.

For the two examples studied in this report, unstable WCU representations were straightforwardly constructed. To impose stability, different construction procedures were proposed. The three most promising are the following: 1) an all-pass $\hat{\Delta}_u$ with possibly large differences between its phase and the phase of the WCU data, 2) a minimum-phase $\hat{\Delta}_u$ with its phase closely matching the data, but with possibly too small magnitude, and 3) a $\hat{\Delta}_u$ which perfectly matches the data points, but with possibly high order and undesirable behavior inbetween data points.

An active suspension control problem was used to evaluate the IO selection method. For this application, WCU construction 3) could not be used due to numerical problems. Construction 2) appeared too small and was useless for IO selection. Therefore, IO selection was performed for construction 1). Depending on the RP test level, many nonviable IO sets were accepted, *i.e.*, the IO selection was not selective. For the specific problem, the IO selection appeared to be more effective if the WCU representation was scaled up, or, equivalently, if the RP requirement was strengthened. However, it is not clear if this tendency is general. The IO selection method appeared to be considerably more efficient than IO selection based on μ-synthesis. By suitably combining the necessity-based IO selection method employing the WCU with the sufficiency-based method from [15,18] and μ-synthesis, an effective IO selection approach results, which may also be more efficient than IO selection based on μ-synthesis.

Bibliography

[1] Gary J. Balas, John C. Doyle, Keith Glover, Andy Packard, and Roy Smith. *μ-Analysis and synthesis toolbox.* The MathWorks, Natick, MA, November 1995. version 3.0.

[2] Joseph A. Ball, Israel Gohberg, and Leiba Rodman. *Interpolation of rational matrix functions*, volume 45 of *Operator theory: Advances and applications.* Birkhäuser Verlag, Basel, 1990.

[3] John C. Doyle, Bruce A. Francis, and Allen R. Tannenbaum. *Feedback control theory.* Mac Millan Publishing Company, New York, 1992.

[4] Pascal Gahinet and Pierre Apkarian. A linear matrix inequality approach to $\mathcal{H}_\infty$ control. *Int. J. Robust and Nonlinear Control*, 4(1):421–448, 1994.

[5] Richard G. Hakvoort. *CURVEFIT*, October 1994.

[6] Richard G. Hakvoort and Paul M. J. van den Hof. Frequency domain curve fitting with maximum amplitude criterion. *Int. J. Control*, 60(5):809–825, November 1994.

[7] Thomas P. Krauss, Loren Shure, and John N. Little. *Signal processing toolbox.* The MathWorks, Natick, MA, June 1994. version 3.0b.

[8] Jay H. Lee, Richard Dean Braatz, Manfred Morari, and Andrew Packard. Screening tools for robust control structure selection. *Automatica*, 31(2):229–235, February 1995.

[9] Jan M. Maciejowski. *Multivariable feedback design.* Addison-Wesley, Amsterdam, 1989.

[10] Andy Packard and John C. Doyle. The complex structured singular value. *Automatica*, 29(1):71–109, 1993.

[11] Andy Packard, Michael K. H. Fan, and John Doyle. A power method for the structured singular value. In *Proc. of the 27th Conf. on Decision and Control*, volume 3, pages 2132–2137, Austin, TX, December 1988.

[12] Patrick Philips, Marc van de Wal, and Bram de Jager. Selection of sensors and actuators based on a necessary condition for robust performance. In *Proc. of the European Control Conf.*, Brussels, Belgium, July 1997.

[13] Sigurd Skogestad and Ian Postlethwaite. *Multivariable feedback control: Analysis and design.* John Wiley & Sons, Chichester, UK, 1996.

[14] Marc van de Wal. Input output selection based on nominal performance and robust stability against unstructured uncertainties: An active suspension application. Technical Report WFW 96.005, Fac. of Mechanical Engineering, Eindhoven University of Technology, January 1996.

[15] Marc van de Wal. Input output selection based on robust performance: An active suspension application. Technical Report WFW 96.048, Fac. of Mechanical Engineering, Eindhoven University of Technology, April 1996.

[16] Marc van de Wal and Bram de Jager. Control structure design: A survey. In *Proc. of the 1995 American Control Conference*, volume 1, pages 225–229, Seattle, WA, June 1995.

[17] Marc van de Wal and Bram de Jager. Selection of sensors and actuators for an active suspension control problem. In *Proc. of the 1996 IEEE Internat. Conf. on Control Applications*, pages 55–60, Dearborn, MI, September 1996.

[18] Marc van de Wal and Bram de Jager. Selection of sensors and actuators based on a sufficient condition for robust performance. In *Proc. of the European Control Conf.*, Brussels, Belgium, July 1997.

[19] Peter M. Young. Controller design with real parametric uncertainty. *Int. J. Control*, 65(3):469–509, October 1996.

[20] Peter M. Young, Matthew P. Newlin, and John C. Doyle. Computing bounds for the mixed μ problem. *Int. J. Robust and Nonlinear Control*, 5(6):573–590, October 1995.

[21] Kemin Zhou, John C. Doyle, and Keith Glover. *Robust and optimal control.* Prentice-Hall, Upper Saddle River, NJ, 1996.

Acknowledgments:

Thanks to Maarten Steinbuch for the suggestion to study the prospects of the "worst case uncertainty" for IO selection. Also thanks to Bram de Jager, Onur Toker, and Anton Stoorvogel for some helpful discussions.